AD NUMBER

**AD820649**

LIMITATION CHANGES

TO:

**Approved for public release; distribution is unlimited.**

FROM:

**Distribution authorized to U.S. Gov't. agencies and their contractors;
Administrative/Operational Use; JUL 1967. Other requests shall be referred to Air force Materials Lab., Wright-Patterson AFB, OH 45433.**

AUTHORITY

**AFML ltr 22 Aug 1968**

AFML-TR-65-2
PART II, VOLUME XIV

# TERNARY PHASE EQUILIBRIA IN TRANSITION METAL-BORON-CARBON-SILICON SYSTEMS

## PART II. TERNARY SYSTEMS
## VOLUME XIV. THE HAFNIUM-IRIDIUM-BORON SYSTEM

*C. E. BRUKL*
*E. RUDY*

*AEROJET-GENERAL CORPORATION*

TECHNICAL REPORT No. AFML-TR-65-2, PART II, VOLUME XIV

JULY 1967



AIR FORCE MATERIALS LABORATORY
DIRECTORATE OF LABORATORIES
AIR FORCE SYSTEMS COMMAND
WRIGHT-PATTERSON AIR FORCE BASE, OHIO

## NOTICE

When Government drawings, specifications, or other data are used for any purpose other than in connection with a definitely related Government procurement operation, the United States Government thereby incurs no responsibility nor any obligation whatsoever; and the fact that the Government may have formulated, furnished, or in any way supplied the said drawings, specifications, or other data, is not to be regarded by implication or otherwise as in any manner licensing the holder or any other person or corporation, or conveying any rights or permission to manufacture, use, or sell any patented invention that may in any way be related thereto.

Copies of this report should not be returned unless return is required by security considerations, contractual obligations, or notice on a specific document.

400 - August 1967 - CO455 - 5-117

# TERNARY PHASE EQUILIBRIA IN TRANSITION METAL-BORON-CARBON-SILICON SYSTEMS

## PART II. TERNARY SYSTEMS
## VOLUME XIV. THE HAFNIUM-IRIDIUM-BORON SYSTEM

*C. E. BRUKL*

*E. RUDY*

# FOREWORD

The research described in this report was carried out at the Materials Research Laboratory, Aerojet-General Corporation, Sacramento, California, under USAF Contract No. AF 33(615)-1249. The contract was initiated under Project No. 7350, Task No. 735001, and was administered under the direction of the Air Force Materials Laboratory, Research and Technology Division with Lt. P.J. Marchiando acting as Project Engineer and Dr. E. Rudy, Aerojet-General Corporation, as Principal Investigator. Professor Dr. H. Nowotny, University of Vienna, served as consultant to the project.

The project, which includes the experimental and theoretical investigations of ternary and related binary systems in the system classes $Me_1$-$Me_2$-C, Me-B-C, $Me_1$-$Me_2$-B, Me-Si-B and Me-Si-C, was initiated on 1 January 1964. An extension effort to this contract commenced in January 1966.

The phase diagram work on the two binary and one ternary systems described in this report, was carried out by C. E. Brukl and E. Rudy. Assisting in these investigations were: D. Harmon (preliminary investigations), E. Spencer (sample preparation), J. Hoffman (metallographic preparations), and R. Cobb (X-ray exposures and photographic work).

Chemical analysis of the alloys was performed under the supervision of Mr. W. E. Trahan, Quality Control Division of Aerojet-General Corporation. The authors wish to thank Mr. R. Cristoni for the preparation of the illustrations, and Mrs. J. Weidner, who typed the report.

The manuscript of this report was released by the authors March, 1967 for publication as an RTD Technical Report.

Other reports issued under USAF Contract AF 33(615)-1249 have included:

Part I. Related Binaries

| | |
|---|---|
| Volume I. | Mo-C System |
| Volume II. | Ti-C and Zr-C Systems |
| Volume III. | Systems Mo-B and W-B |
| Volume IV. | Hf-C System |
| Volume V. | Ta-C System. Partial Investigations in the Systems V-C and Nb-C |
| Volume VI. | W-C System. Supplemental Information on the Mo-C System |
| Volume VII. | Ti-B System |
| Volume VIII. | Zr-B System |
| Volume IX. | Hf-B System |
| Volume X. | V-B, Nb-B, and Ta-B Systems |
| Volume XI | Final Report on the Mo-C System |

Part II. Ternary Systems

| | |
|---|---|
| Volume I. | Ta-Hf-C System |
| Volume II. | Ti-Ta-C System |
| Volume III. | Zr-Ta-C System |
| Volume IV. | Ti-Zr-C, Ti-Hf-C, and Zr-Hf-C Systems |
| Volume V. | Ti-Hf-B System |
| Volume VI. | Zr-Hf-B System |
| Volume VII. | Systems Ti-Si-C, Nb-Si-C, and W-SiC |
| Volume VIII. | Ta-W-C System |
| Volume IX. | Zr-W-B System. Pseudo-Binary System $TaB_2$-$HfB_2$ |
| Volume X. | Systems Zr-Si-C, Hf-Si-C, Zr-Si-B, and Hf-Si-B |
| Volume XI. | Systems Hf-Mo-B and Hf-W-B |
| Volume XII. | Ti-Zr-B System |
| Volume XIII. | Phase Diagrams of the Systems Ti-B-C, Zr-B-C, and Hf-B-C. |

Part III. Special Experimental Techniques

| | |
|---|---|
| Volume I. | High Temperature Differential Thermal Analysis |
| Volume II. | A Pirani-Furnace for the Precision Determination of the Melting Temperatures of Refractory Metallic Substances |

Part IV. Thermochemical Calculations

| | |
|---|---|
| Volume I. | Thermodynamic Properties of Group IV, V, and VI Binary Transition Metal Carbides. |
| Volume II. | Thermodynamic Interpretation of Ternary Phase Diagrams |
| Volume III. | Computational Approaches to the Calculation of Ternary Phase Diagrams. |

This technical report has been reviewed and is approved.

W. G. RAMKE
Chief, Ceramics and Graphite Branch
Metals and Ceramics Division
Air Force Materials Laboratory

## ABSTRACT

Constitution diagrams of the binary hafnium-iridium and iridium-boron systems as well as an isothermal section of the hafnium-iridium-boron ternary system have been established by means of Pirani melting point investigations, metallography, Debye-Scherrer X-ray, and chemical analysis.

There are three intermediate phases, $Ir_3B_2$, $IrB_{0.89}$, and $IrB_{1.50}$ in the rather low melting iridium-boron system which contains four eutectics.

$Hf_2Ir$, $Hf_3Ir_2$, $HfIr_{1-x}$, HfIr, $HfIr_{1+x}$, and $HfIr_3$ are the phases present in the hafnium-iridium system. The highest melting phase in this system is $HfIr_3$ whose melting point is 2460°C. The phase relationships in the central portion of the binary system are quite complex.

The ternary hafnium-iridium-boron system has five ternary phases: $Hf_{.32}Ir_{.46}B_{.22}$, $Hf_{.19}Ir_{.49}B_{.32}$, $Hf_{.07}Ir_{.51}B_{.42}$, $Hf_{.07}Ir_{.42}B_{.51}$, and $Hf_{.02}Ir_{.60}B_{.38}$. $HfIr_3$ has an extended solubility for boron. $HfB_2$, which does not form a two-phase equilibrium with iridium, exhibits no solubility into the ternary field.

High temperature application possibilities for hafnium-iridium-boron composite borides are briefly discussed.

TABLE OF CONTENTS

TABLE OF CONTENTS (Cont'd)

## ILLUSTRATIONS

ILLUSTRATIONS (Cont'd)

## TABLES

# I. INTRODUCTION AND SUMMARY

## A. INTRODUCTION

Hafnium diboride is the most oxidation resistant boride known to date[1], and zirconium diboride is almost as good; but, the most serious inherent drawback preventing widespread use of these diborides is their susceptibility to mechanical failure under thermal stress. One of the scientific and developmental goals of high temperature materials research is to find an alloying element or compound for use as a binder which would permit the use of these diborides at high temperatures in an oxidizing environment.

A suitable binder must not detract too greatly from the oxidation resistance, but far more important, must not react with the parent diboride to form temperature dependent, extended solid solutions or form intermediate ternary compounds.

The good oxidation resistance of several of the platinum group metals is well documented, and some of these elements are quite refractory. There is, however, practically nothing known about the phase relationships or compatibility of hafnium and zirconium diborides with the platinum-group metals. A basic delinearization of the phase relationships in such ternary systems, (Hf or Zr)-(Platinum-Group Metal)-(Boron), is necessary prior to the undertaking of any possible oxidation studies.

The main interest in the phase investigations concentrated on determining whether or not the refractory diborides form stable two-phase equilibria with platinum-group metals or suitable binary platinum-metal containing alloys. Cursory investigations in the ternary boride systems with osmium, rhodium, platinum, and iridium in combination with zirconium and hafnium showed that such equilibria with the refractory diborides do not exist. Numerous ternary phases are formed, and the phase relationships are very complex. Since neither the time available nor the funding for these expensive

materials were sufficient to permit the extensive investigation of all of these combinations, and further because the data from the respective binary systems are so scarce; only one ternary system, Hf-Ir-B, was selected for detailed investigation. The results of the examination of the Hf-Ir-B system should yield much helpful information in future detailed studies of the other ternary boride combinations in this system class.

## B. SUMMARY

### 1. Hafnium-Iridium

The hafnium-iridium binary system was investigated by means of metallography, Pirani melting point experiments, and Debye-Scherrer X-ray analysis.

Figure 1 shows the hafnium-iridium binary system. Three new phases $Hf_3Ir_2$, $HfIr_{1+x}$, and $HfIr_{1-x}$ were found; the three phases $Hf_2Ir$, HfIr, and $HfIr_3$ were confirmed. Of the six phases, the crystal structures of only $Hf_2Ir$ and $HfIr_3$ are known.

$Hf_2Ir$, which has only a very slight homogeneous range, decomposes peritectically at 1775 $\pm$ 30°C; the lattice parameter of this $Ti_2Ni$ isomorphous phase is $12.32_3$ Å.

$Hf_3Ir_2$, which likewise has only a narrow homogeneous range, decomposes peritectically at 1970 $\pm$ 20°C. A somewhat tentative description is given for the equilibria in the portion of the diagram from 48 to 52 At.% Ir: three phases are present: HfIr, with a simple, but as yet unknown crystal structure, melts congruently at 2410 $\pm$ 30°C and decomposes eutectoidally into $HfIr_{1-x}$ and $HfIr_{1+x}$ at about 1400°C. The $HfIr_{1-x}$ phase decomposes in a peritectoid reaction into $Hf_3Ir_2$ and HfIr at approximately 1900°C; the $HfIr_{1+x}$ phase also undergoes a peritectoid decomposition into $HfIr_3$ and HfIr at about 2050°C.

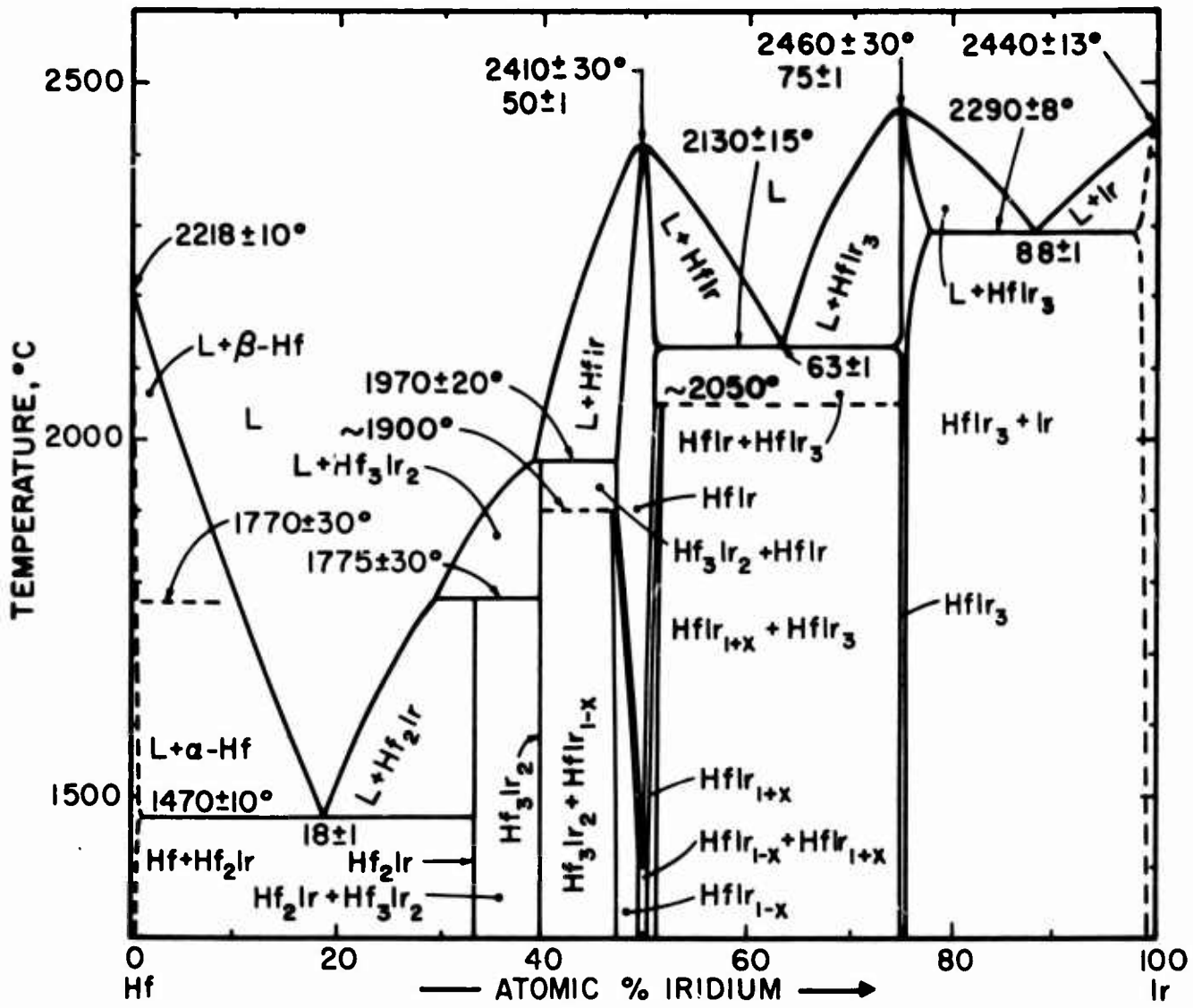


Figure 1. The Hafnium-Iridium Binary System

The $HfIr_3$ phase, which has the ordered $Cu_3Au$ type structure, melts congruently at 2460 ± 30°C; the lattice parameters of this phase which has a small homogeneous range, vary between $3.89_5$ and $3.93_1$ Å.

There are three eutectics in the hafnium-iridium system: between Hf and $Hf_2Ir$ at 18 ± 1 At.% iridium and 1470 ± 10°C; between HfIr and $HfIr_3$ at 63 ± 1 At.% iridium and 2130 ± 15°C; and between $HfIr_3$ and Ir at 88 ± 1 At.% iridium and 2290 ± 8°C.

## 2. Iridium-Boron

The iridium-boron binary system was also investigated by means of Pirani melting point experiments, metallography, and Debye-Scherrer X-ray analysis; the composition of the experimental alloys was ascertained by chemical analysis.

Figure 2 shows the constitution diagram of the iridium-boron system.

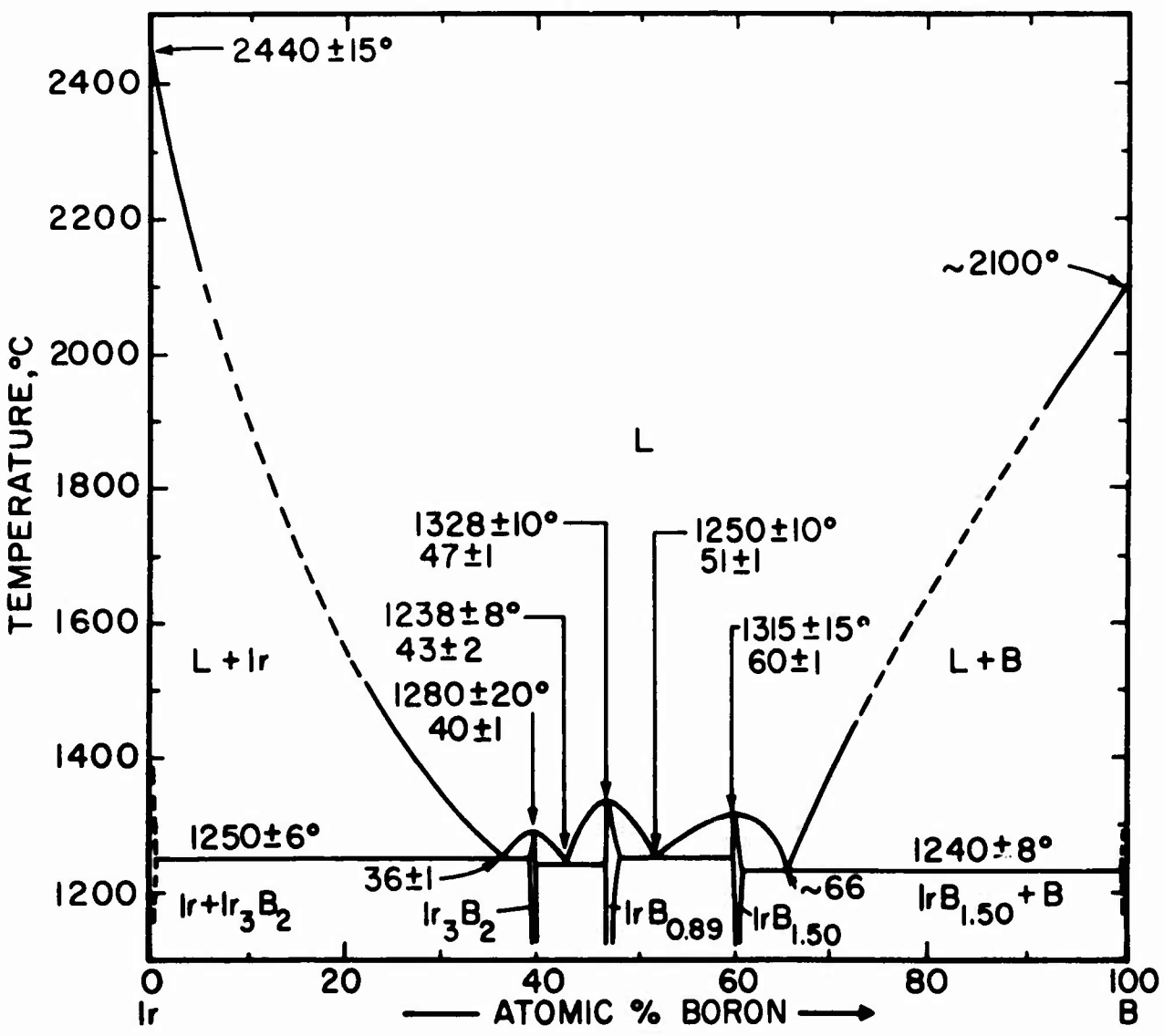


**Figure 2. The Iridium-Boron Binary System**

There are three intermediate phases, $Ir_3B_2$, $IrB_{0.89}$, and $IrB_{1.50}$. The first two named phases had been previously described, but the structure of $Ir_3B_2$ is unknown, and the composition of the phase near the monoboride composition was uncertain. The $IrB_{150}$ phase was apparently previously observed, but its composition reported at 67 At.% B. The crystal structure of $Ir_3B_2$ and $IrB_{1.50}$ are as yet unsolved.

The $Ir_3B_2$ phase has a very narrow homogeneous range, whereas the $IrB_{0.89}$ and $IrB_{150}$ have somewhat larger homogeneous areas. All three intermediate phases melt congruently: $Ir_3B_2$ at 1280 $\pm$ 20°C; $IrB_{0.89}$ at 1328°C; and $IrB_{1.50}$ at 1315°C. There are four eutectics in this system: between Ir and $Ir_3B_2$ at 36 $\pm$ 1 At.% B and 1250 $\pm$ 6°C; between $Ir_3B_2$ and $IrB_{0.89}$ at 43 $\pm$ 2 At.% B and 1280 $\pm$ 20°C; between $IrB_{0.89}$ and $IrB_{150}$ at 51 $\pm$ 1 At.% B and 1250 $\pm$ 10°C; and between $IrB_{1.50}$ and boron at about 66 At.% B and 1240 $\pm$ 8°C.

## 3. Hafnium-Iridium-Boron

An isothermal section of this ternary system was investigated primarily by studying X-ray powder patterns of a great number of ternary alloys.

Figure 3 presents the isothermal section of this ternary system at 1100°C. Five ternary phases are present; their compositions expressed in mole fractions of the individual compounds are: $Hf_{.32}Ir_{.46}B_{.22}$ $Hf_{.19}Ir_{.49}B_{.32}$, $Hf_{.07}Ir_{.51}B_{42}$, $Hf_{07}Ir_{42}B_{.51}$, and $Hf_{.02}Ir_{.60}B_{.38}$.

The main features of the ternary system are as follows: $HfB_2$ forms two-phase equilibria with three of these ternary phases as well as with $Hf_2Ir$, $Hf_3Ir_2$, HfIr, $HfIr_3$(B) and $IrB_{1.50}$; hafnium diboride exhibits no solubility into the ternary system. The $HfIr_3$(B) solid solution takes about 15 mole % boron into solution at 1100°C and about 24 mole % at temperatures just below solidus temperatures; this phase forms two-phase equilibria with $Hf_{.32}Ir_{.46}B_{22}$, $HfB_2$, $Hf_{.19}Ir_{.49}B_{.32}$, $Hf_{.07}Ir_{.51}B_{.42}$, $IrB_{0.89}$,

and $Ir_3B_2$. The iridium metal phase is in equilibrium with only its respective neighboring binary phases and $Hf_{.02}Ir_{.60}B_{.38}$; it shows only slight solubilities for boron and hafnium.

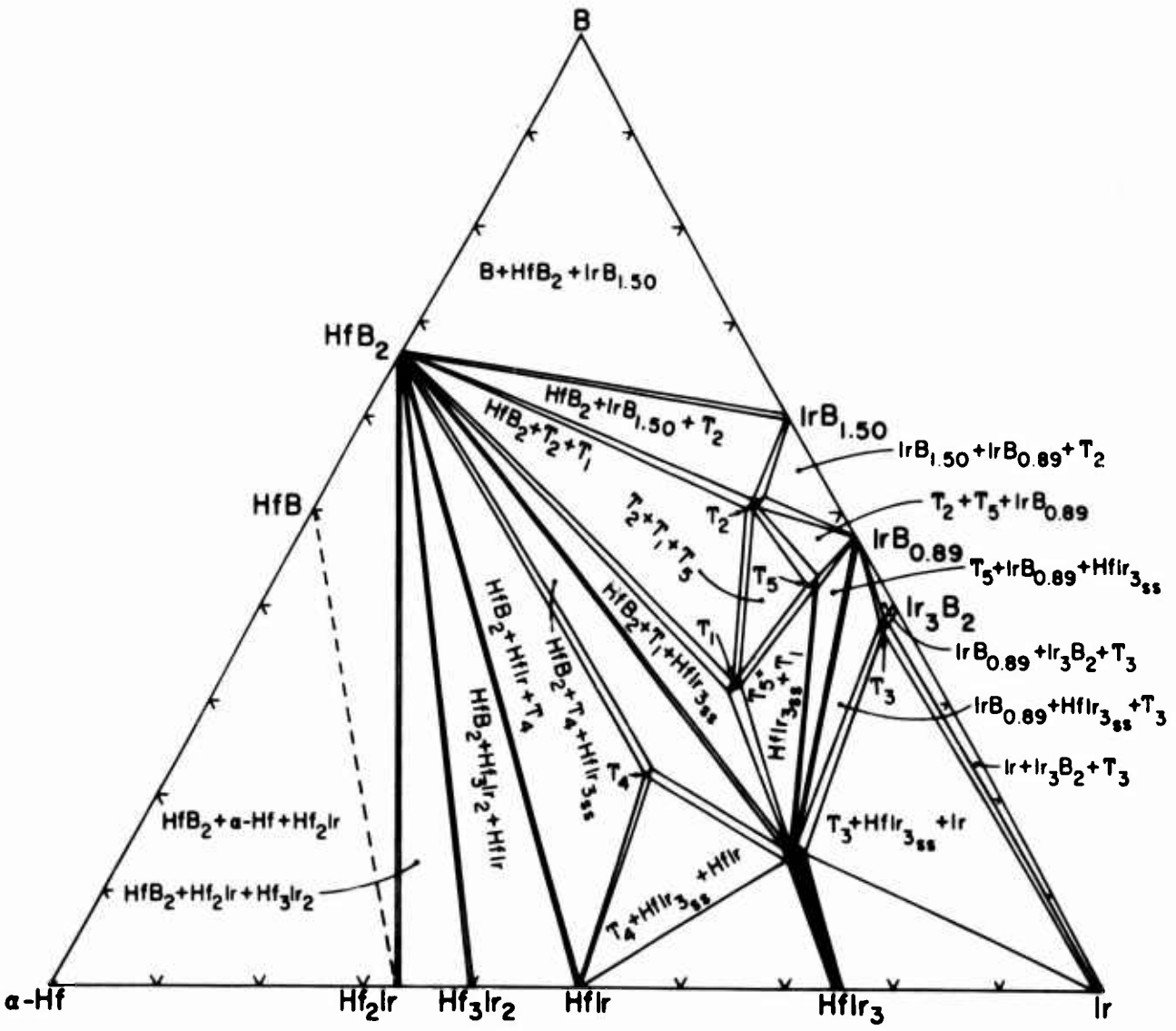


Figure 3. The Hafnium-Iridium-Boron System at 1100°C.

4. Other (Hafnium, Zirconium)-(Platinum-Group Metal)-Boron Ternary Combinations

Cursory investigations in the systems Zr-Rh-B, Hf-Rh, B, Zr-Pt-B, Hf-Pt-B, Zr-Os-B, Hf-Os-B, and Zr-Ir-B showed a two-phase equilibrium $ZrB_2$ or $HfB_2$-Platinum-Group Metal does not exist

in any of these systems. There are numerous ternary phases formed in all of these ternary systems, and the phase relationships are very complex.

## II. LITERATURE REVIEW

### A. BOUNDARY SYSTEMS

#### 1. Hafnium-Iridium

There has been no extensive work on the complete hafnium-iridium binary system, although isolated phases have been discovered and, in part, structurally described.

Nevitt and Schwartz[2], in a study seeking $Ti_2Ni$-type phases in zirconium and hafnium binary systems, found a $Hf_2Ir$ phase at 30 At.% Ir with this structure; the lattice parameter was 12.352 Å. In an investigation concerned with the formation of equatomic alloys, A.E. Dwight[3] found that the alloys which occur near HfIr do not possess either a body centered cubic or the CsCl type structure. This same author, in a publication with P.A. Beck[4], found that $HfIr_3$ crystallizes in the $Cu_3Au$ ordered structure with the lattice parameter: 3.935 Å. Due to the lack of any great difference in the atomic scattering factors of hafnium and iridium, no superlattice lines were observed[4] for the ordered $HfIr_3$ phase.

Table 1 shows the observed hafnium iridides and their crystal structures.

Table 1. Intermediate Hafnium-Iridium Phases and Their Crystal Structures

| Phase | Crystal Structure | Lattice Parameter | Ref. |
|---|---|---|---|
| $Hf_2Ir$ | Cubic $Ti_2Ni$ type | 12.352Å | 2 |
| HfIr | Unknown | | 3 |
| $HfIr_3$ | Cubic $Cu_3Au$ type | 3.935Å | 4 |

## 2. Iridium-Boron

No complete investigation has been performed on the iridium-boron binary system, although the majority of the other platinum-metal boron systems has been the object of considerable attention, especially in the field of crystal structural investigations.

The first iridium-borides were prepared and described by J. H. Buddery and A.J.E. Welch[5]; using X-ray techniques, these authors found three phases at the approximate compositions given by the formulae: $Ir_3B_2$, IrB, and $IrB_2$. Using a hot stage microscope, G. Reinacher[6] found that a eutectic exists between iridium and the first boride at 1046°C. The author, however, mentioned the fact that the melting points observed were probably lowered by magnesium and silicon contaminations. B. Aronsson, E. Stenberg, and J. Åselius[7, 8], in two publications, have said that the composition of the iridium monoboride phase is $IrB_{\sim 1.1}$, and that this phase is isomorphous with the tetragonal $ThSi_2$; the lattice parameters given were: $a = 2.81_0$ and $c = 10.26_3$ Å. They[7] further stated that the solubility of boron in iridium is quite small.

Reference[9] has been made to the fact that a compound of the composition $IrB_{1-2}$ has the $AlB_2$ (C-32) type structure, but this supposition has not been substantiated.

Table 2 lists the observed iridium borides and their crystal structures.

Table 2. Intermediate Iridium-Boron Phases and their Crystal Structures

| Phase | Crystal Structure | Lattice Parameter | Ref. |
|---|---|---|---|
| $Ir_3B_2$ | Unknown | | 5 |
| $IrB(IrB_{\sim 1.1})$ | Tetragonal, $ThSi_2$ type | $a=2.81_0$ and $c=10.26_3$ Å | 7, 8 |
| $IrB_2$ | Unknown | | 5 |
| $IrB_{1-2}$ | Hexagonal, C-32 type (?) | $a=2.81_0$ and $c=10.27$ Å | 9 |

### 3. Hafnium-Boron

Two intermediate phases are formed in the Hf-B system. $HfB_2$, which crystallizes in a hexagonal lattice structure, has a negligible homogeneous range and has been reported to melt in the temperature range 3060° - 3240°C[10, 11-13].

Early investigations[11] indicated that a monoboride with a face-centered cubic structure was formed in the Hf-B system. However, it was later shown by E. Rudy and F. Benesovsky[14] that the true structure of the monoboride is an orthorhombic B-27 type; the occurrence of the previously observed face-centered cubic phase is attributed to impurities such as carbon, nitrogen, and oxygen.

Proposed phase diagrams[15, 16], for the Hf-B system have been based mainly on estimates. A publication by Kafuman and Clougherty[1] has reported a Hf-HfB eutectic temperature of 1960°C as well as a peritectic decomposition temperature of greater than 2400°C for HfB. For earlier details, including the preparation of hafnium borides, Hartstoffe[17] by Kieffer and Benesovsky should be consulted. A complete investigation

of the hafnium-boron system was carried out in this laboratory[18]. The results are depicted in Figure 4. The solubility of boron in β-hafnium is less than 2 At.% B; the eutectic between β-Hf and Hf-B, whose temperature is 1880°C, lies at about 13 At.%.

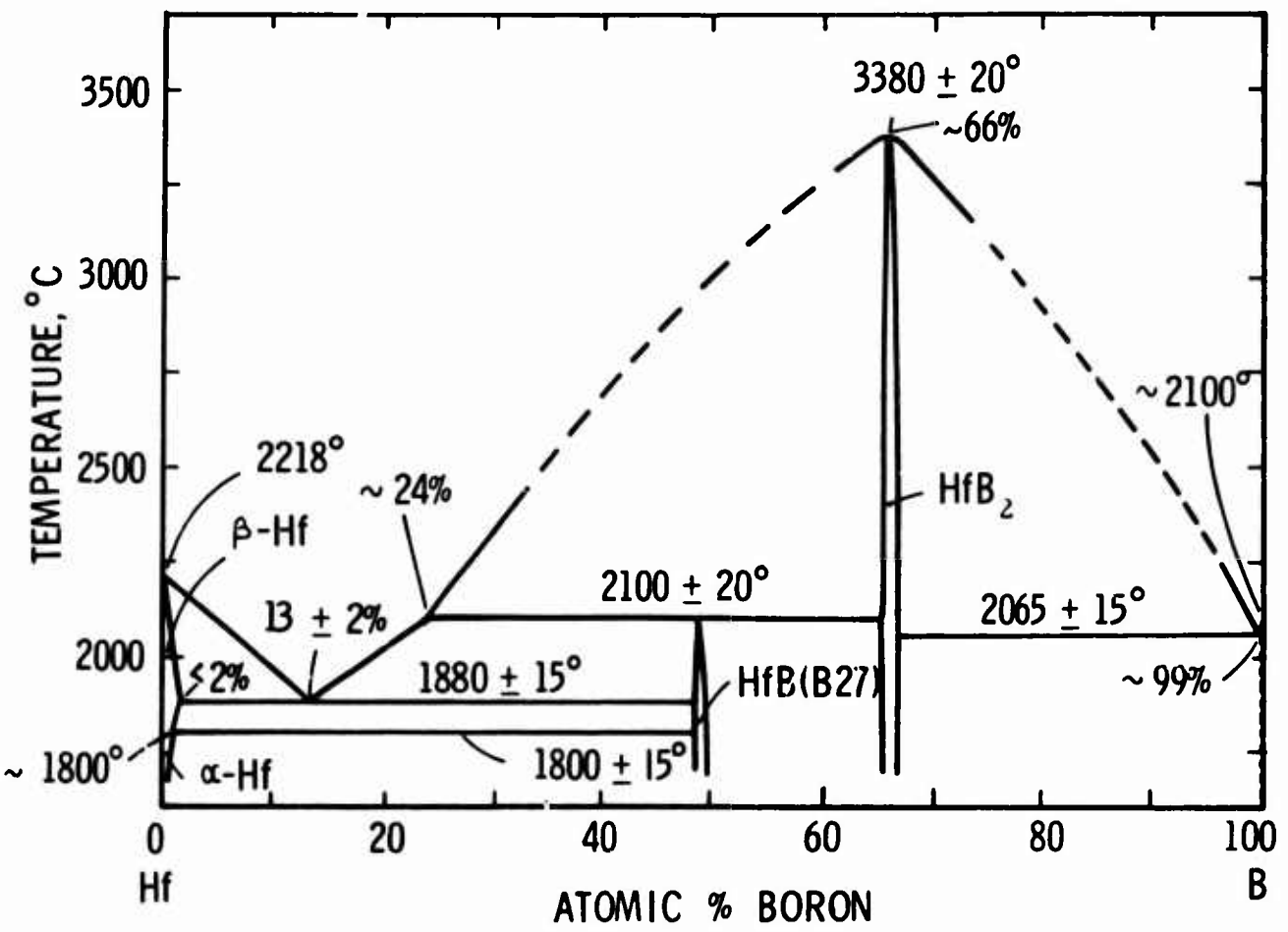


Figure 4. The Hafnium-Boron Constitution Diagram.
(E. Rudy and St. Windisch, 1966)

HfB, with an orthorhombic unit cell, decomposes peritectically into melt and $HfB_2$ at 2100°C. $HfB_2$ melts congruently at 3380°C and forms a eutectic with boron at about 99 At.% B. The eutectic temperature is 2065°C.

Table 3 gives the intermediate phases and crystal structures of the Hf-B compounds.

Table 3. Lattice Parameters and Crystal Structures of Intermediate Hf-B Compounds

| Phase | Crystal Structure | Lattice Parameters | Ref. |
|---|---|---|---|
| $HfB_2$ | Hexagonal (C-32 type) | a = 3.142 Å<br>c = 3.447 Å | 19 |
| HfB | Orthorhombic (B-27 type) | a = 6.51$_7$ Å<br>b = 3.21$_8$ Å<br>c = 4.92$_0$ Å | 19 |

## B. TERNARY SYSTEM

### 1. Hafnium-Iridium-Boron

There are no reported investigations in the literature concerning the hafnium-iridium-boron system.

# III. EXPERIMENTAL PROGRAM

## A. STARTING MATERIALS

Elemental metal and boron powders, as well as pre-prepared hafnium diboride and iridium monoboride powders were used as the starting materials for these investigations.

### 1. Hafnium

The hafnium powder, supplied by the Wah Chang Corp., Albany, Oregon had the following main impurities as given by the vendor (in ppm): Al-27, C-30, Nb-<100, Cu-<40, Fe-<70, H-35, N-57, O-550,

Si-<40, Ta-<200, Ti-55. and Zr-2.77 Wt.%; this material was sized less than 74 micrometers. The lattice parameters of this hafnium metal as measured from a $CuK_\alpha$ Debye-Scherrer powder patterns were a = $3.19_5$ and c = $5.05_5$ Å.

2. Iridium

The iridium metal powder was supplied by Englehard Industries, Inc., Newark, New Jersey and had the following major impurities as listed by the vendor (in ppm): Pt-<200, Rh-510, Pd-<200, Cu-78, Pd-100, Fe-<100, Si-26, Ca-45, and Sb-<15. The particle size of this powder was smaller than 44 micrometers. The lattice parameter of this iridium powder taken from a $CuK_\alpha$ powder pattern was $3.839_3$ Å.

3. Boron

The boron used was supplied by the United Mineral and Chemical Corporation, New York and was guaranteed 99% minimum purity; the vendor's analysis was (in ppm): Fe-2500 and C-800. An in-plant analysis of this material yielded the following results (in ppm): Mn-1500, Si-2000, Cr-1000, Mo-3000, Ni-500, Cu-800, Al-1000, Fe-5000, Ti-1000, Mg-20, Ca-50, and 1.37 Wt.% $B_2O_3$. The particles of this boron powder ranged in size between 149 and 44 microns.

4. Hafnium Diboride

Hafnium diboride was prepared by direct combination of the elements at high temperatures. In order to circumvent difficulties arising from the violent reaction in the formation of the diboride, a master alloy containing 85 atomic percent boron was prepared first. This intermediate product was then comminuted, the necessary amount of hafnium powder admixed, and again reacted for 2 hours at 1800° to 2000°C under a high purity helium atmosphere. After cooling under vacuum, and discarding of the zones adjacent to the tantalum container, the reaction lumps were

crushed and comminuted in carbide-lined ball mill jars to a particle size smaller than 60 micrometers. Cobalt traces, which were picked up during grinding, were removed by an acid-leach in an 8N mixture of hydrochloric and sulfuric acid. The final powder product had a boron content of 11.19 Wt.% boron (67.6 At.%); the carbon content of this hafnium diboride was approximately 110 ppm. The lattice parameters were: a = 3.142 and c - 3.477 Å.

### 5. Iridium Monoboride

A small amount of iridium monoboride with a nominal composition of 50 At.% boron was prepared for the investigation of the Ir-B binary system and for isolated samples in the Hf-Ir-B ternary system. The appropriate amounts of iridium and boron powder were mixed by hand, cold pressed into pellets, and arc melted under high purity helium in a Zak tungsten electrode button arc melter. The small oxygen impurity removed from sample was visible as a white ring of $B_2O_3$ on the cold surface of the copper hearth. The buttons were then crushed and ground by hand to a particle size less than 74 micrometers. No chemical analysis of the boron content of this small amount of master alloy was performed, but several of the subsequent Ir-B alloys were analyzed in triplicate. An Debye-Scherrer X-ray, taken with $CuK_\alpha$ radiation showed a single phase monoboride with the $ThSi_2$ structure.

## B. ALLOY PREPARATION AND HEAT TREATMENT

### 1. Hafnium-Iridium

The binary hafnium-iridium alloys for Pirani melting point experiments and subsequent studies were prepared by cold pressing (2000 psi) the small samples in a contoured split die arrangement with a retractable pin used for the black body hole. Figure 5 shows one of these pressed samples.

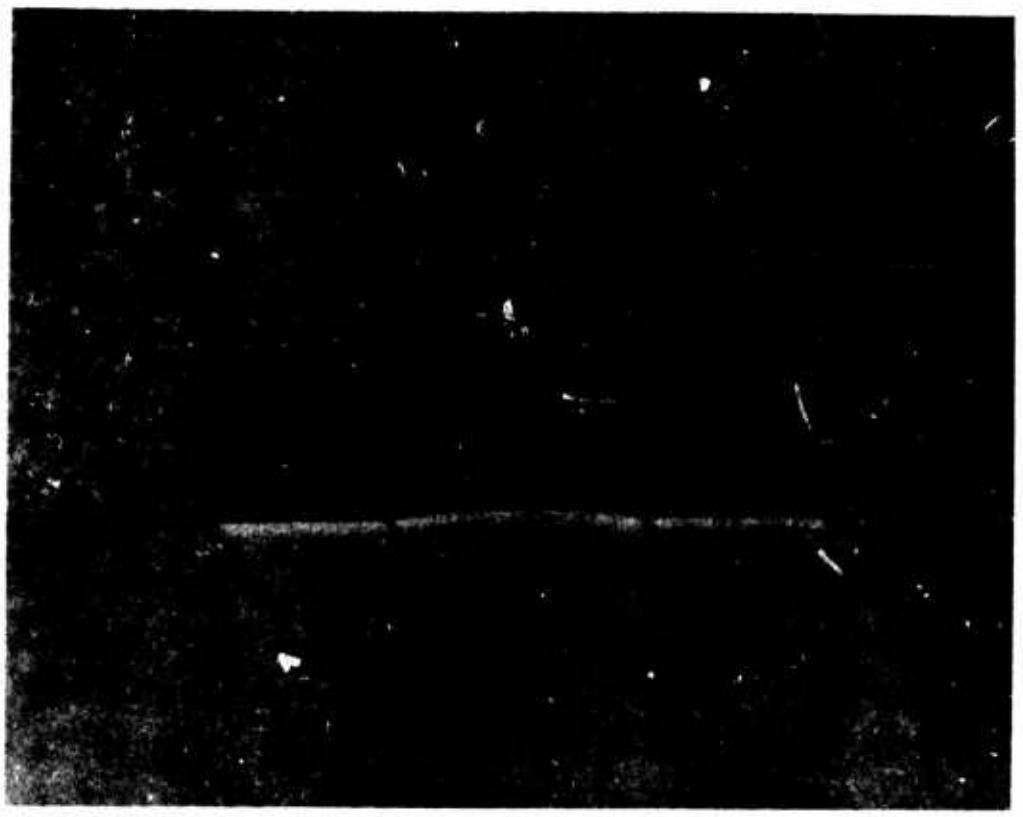

Figure 5. Cold Pressed Pirani Melting Point Specimen

A strengthening heat treatment of the green compacts was carried out at 1225°C for two hours in a vacuum of $< 1 \times 10^{-5}$ Torr. The contact zone of the hafnium-iridium samples with the tantalum can was carefully removed to avoid possible contamination.

After the melting point experiments were run, the deformed samples (with the ends cleaned off to avoid possible tungsten contamination) were arc melted under high purity helium in a Zak button arc melter. The larger portion of each of these arc melted samples was given a heat treatment of 63 hours at 1460°C under a vacuum of $1 \times 10^{-5}$ Torr. Some of the arc melted samples were heat treated for 72 hours at 1150°C under high vacuum. Portions of the arc melted samples, as well as the samples receiving the heat treatments were ground to powder and used for Debye-Scherrer X-ray powder patterns . Several of the more ductile alloy powders were annealed under vacuum at 1100°C. The arc melted samples were mounted and studied metallographically.

## 2. Iridium-Boron

Initial attempts at cold pressing mixtures of Ir, IrB, and B were unsuccessful; the small sample mixtures were hot pressed in graphite dies and the outer graphite contact zone carefully removed; the center area was reduced and a black body hole drilled in the Pirani melting point specimen. After the melting point runs, the tungsten platelet contact zone was removed to prevent contamination, and the samples were arc melted under high purity helium. Portions of each of the arc melted specimens were heat treated for 64 hours at 1000°C under static helium. Debye-Scherrer powder photographs as well as metallographic investigations were made of and performed on both the heat treated and arc melted samples.

## 3. Hafnium-Iridium-Boron

The fifty-four alloys used for the investigation of the solid state section of the ternary hafnium-iridium-boron system were made by various means and received various heat treatments. The samples were prepared by hot pressing the elemental powders sometimes with and sometimes without pre-prepared boride master alloys. To insure complete homogenization (there is a great difference in the melting points of the various respective binary phases) many of the alloys were arc melted and subsequently heat treated. Debye-Scherrer powder photographs were made of all heat treated and arc melted alloys to determine the phase equilibria of this ternary system. Table 4 shows the preparation and heat treatment schedule of the hafnium-iridium-boron ternary alloys.

Table 4. Preparation and Heat Treatment Schedule of the Hafnium-Iridium-Boron Ternary Alloys

| Initial Preparation | Intermediate Treatment | Final Heat Treatment |
|---|---|---|
| Preliminary Samples: | | |
| Hot Pressing | Arc Melting | - |
| Hot Pressing | - | 73 hours/1400°C/Helium |
| Hot Pressing | Arc Melting | 73 hours/1400°C/Helium |
| Hot Pressing | Arc Melting | 300 hours/1000°C/ $1 \times 10^{-5}$ Torr |
| Subsequent Samples: | | |
| Cold Pressing | Arc Melting | - |
| Cold Pressing | Arc Melting | 64 hours/1000°C/ $1 \times 10^{-5}$ Torr |

## C. MELTING POINT INVESTIGATION

The melting points of the hafnium-iridium and iridium-boron binary alloys were determined by the previously described Pirani-technique[19, 20]. To minimize metal and boron losses at the higher melting temperatures, the melting point furnace was pressurized with high purity helium at 2-1/4 atmospheres after a short vacuum degassing at sub-solidus temperatures. The temperature measurements were carried out with a disappearing-filament type micropyrometer which was calibrated against a certified, standard lamp from the National Bureau of Standards. The temperature correction for absorption in the quartz furnace window, as well as that correction for deviation due to non-black body conditions, have been amply described and and validated in previous reports[19, 20].

## D. METALLOGRAPHY

Thirty samples in the hafnium-iridium and iridium-boron binary systems were metallographically examined.

The specimens were mounted in an electrically conductive mixture of diallylphtalate-lucite-copper mounting material. Coarse grinding and rough polishing were done on varying grit sizes (120-600) of silicon carbide paper. A fine, highly polished sample surface was ultimately obtained using a suspension of 0.05 micron alumina in a 5% chromic acid solution on microcloth. Etching solutions and techniques varied with the composition of the binary alloys. It was found that the hafnium-iridium samples quite rich in hafnium were best etched with a ten second electroetch process in a 5% sulfuric acid solution; hafnium-iridium samples containing about 55 to 75 At% iridium showed the best results when electroetched in a 20% hydrochloric acid solution saturated with sodium chloride. The iridium-rich hafnium-iridium alloys as well as all the iridium-boron alloys were electroetched in a 2% aqueous solution of sodium hydroxide.

## E. X-RAY ANALYSIS

Debye-Scherrer powder diffraction patterns, using $CrK_a$ and in some instances $CuK_a$ radiation, were made of all samples after arc melting, heat treating, and powder annealing. The exposures were made in a 57.4 mm. camera on a Siemens Crystalloflex II unit, and a Siemens-Kirem coincidence scale with micrometer attachment was used for measuring the films.

## F. CHEMICAL ANALYSIS

Chemical analysis were carried out only for boron in the binary iridium boron system; it was felt that both the hafnium and iridium were of sufficiently high purity; further, since the melting temperatures of

the intermediate compounds are not exceptionally high, compositional shifts due to preferential vaporization of phase components are not expected to occur.

The wet-chemical method used for the boron analysis consists of converting bound or free boron to boric acid, which then — after removal of interfering accompanying elements — is determined by differential titration of the complex acid formed with mannitol. The detailed procedures were analogous to those extensively described in an earlier report[21].

## IV. RESULTS

### A. HAFNIUM-IRIDIUM

Thirty samples were prepared for melting point investigations and subsequently arc melted and/or heat treated; twenty-one samples were examined metallographically and used in conjunction with the Debye-Scherrer X-ray patterns to assist in the establishment of the binary hafnium-iridium phase diagram.

Melting point results and metallographic examinations showed that a eutectic with a melting isotherm of 1470 $\pm$ 10°C is present between hafnium and the hafnium-richest intermediate compound $Hf_2Ir$; the eutectic point is located at 18 $\pm$ 1 At.% iridium. Figure 6 shows a photomicrograph of the eutectic in this region. In confirmation of the findings of Nevitt and Schwartz[2], these investigations have found that the hafnium-richest phase is located close to 33 At% iridium and possesses the cubic $Ti_2Ni$ structure; the lattice parameter determined was $12.32_3$ Å. This intermediate phase has a very narrow homogeneous range; no lattice parameter variation could be detected. The $Hf_2Ir$ phase decomposes peritectically at 1775 $\pm$ 30°C. Figure 7 shows the peritectic formation of the $Hf_2Ir$ phase.

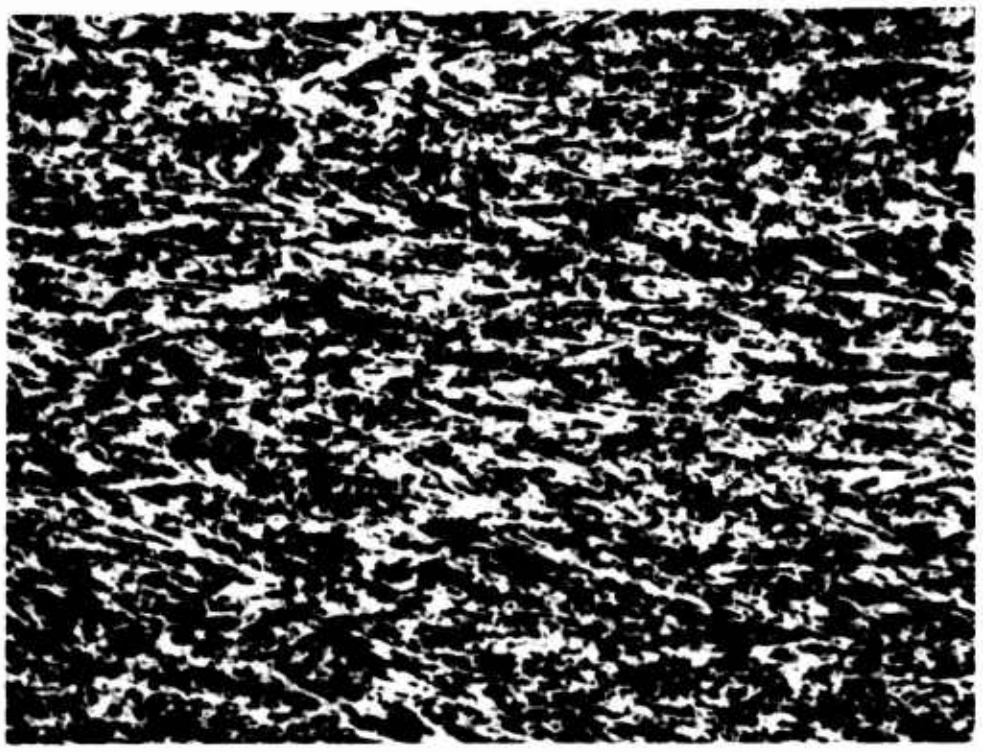

Figure 6. Photomicrograph of a Hf-Ir (81.5-18.5) Arc Melted Alloy X1000
Hf-$Hf_2Ir$ Eutectic.

Figure 7. Photomicrograph of Hf-Ir (67-33) Arc Melted Alloy X600
Peritectic Reaction Mixture.

Remnants of $Hf_3Ir_2$ (Long Grains and Islands) with
Hafnium (not completely resolved) and $Hf_2Ir$.

Roentgenographic and metallographic results showed the presence of a previously unreported, intermediate hafnium-iridium phase very close to the composition of $Hf_3Ir_2$ . The Debye-Scherrer pattern, which has not been indexed as yet, is presented in Table 5. The $Hf_3Ir_2$ phase decomposes peritectically into HfIr and liquid at 1970 $\pm$ 20°C. The X-ray films of this phase show practically no variation in lattice parameter, and therefore, it is to be assumed that its homogeneous range is quite small. Figure 8 shows the formation of $Hf_3Ir_2$ from HfIr and liquid.

Table 5. Diffraction Pattern of the Hf-Ir Phase Near $Hf_3Ir_2$ $CrK_\alpha$ Radiation

| $Sin^2\theta$ | Estimated Intensity | $Sin^2\theta$ | Estimated Intensity |
|---|---|---|---|
| .16673 | 2 | .74240 | 2 diffuse |
| .19701 | 7 | .76020 | 4 diffuse |
| .24069 | 10 | .78104 | 3 diffuse |
| .25318 | 9 | .79431 | 2 diffuse |
| .32522 | 3 | .80631 | 6- |
| .38090 | 2 | .83222 | 3+ |
| .40957 | 4+ | .86603 | 4 |
| .50856 | 3 | .87460 | 6+ |
| .57615 | 7 | .89476 | 1+ diffuse |
| .59369 | 2 | .91780 | 7+ diffuse |
| .61825 | 5 | .93188 | 4 diffuse |
| .66822 | 5 | .95084 | 1 diffuse |
| .70862 | 6+ | .95825 | 4 diffuse |

The phase relationships in the central portion of the hafnium-iridium system between about 48 and 52 atomic percent iridium are rather complicated; it may be said that there are three distinct crystal structures or phases present, although due to the transformations occurring and the

Figure 8. Photomicrograph of an Hf-Ir (60-40) Arc Melted Alloy. Peritectic Reaction Mixture. X600
Islands of $Hf_2Ir$ in $Hf_3Ir_2$-HfIr Mixture (not completely resolved).

resulting lack of attainment of equilibrium, the quality of the Debye-Scherrer X-ray patterns obtained was not sufficiently good to permit a detailed evaluation or listing of the individual crystal structures. Two of the phases occurring show quite complex X-ray patterns, and one is quite simple; this simple pattern is obviously the phase referred to by A. E. Dwight[3] and designated as HfIr. In concurrence with Dwight, it was found that this phase is neither body-centered cubic nor of the CsCl type.

X-ray and metallographic evidence of both heat treated and arc melted samples permitted a tentative description of the phase equilibria in this central portion of the hafnium-iridium phase diagram as shown in Figure 9. The phase previously described by Dwight[3], which exists with a small homogeneous range about HfIr, is stable only at temperatures above about 1400°C; it decomposes in a slow eutectoid reaction into two phases designated as $HfIr_{1+x}$ and $HfIr_{1-x}$ near 1400°C. The HfIr phase was found to

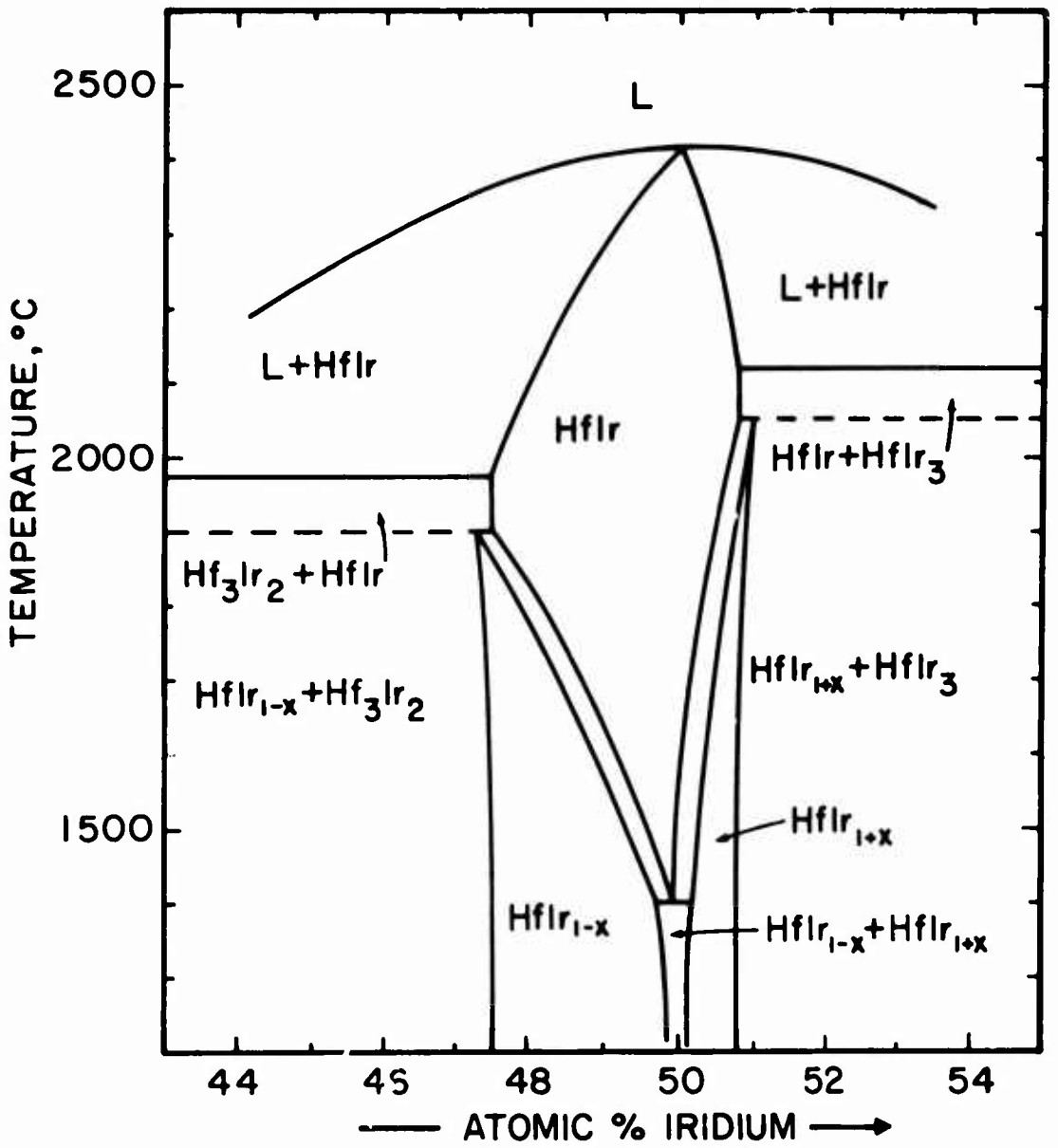


Figure 9. Tentative, Semi-Schematic Diagram of the Region near HfIr.

melt congruently at 2410 ± 30°C. The $HfIr_{1-x}$ phase which exists over a small homogeneous range between about 48 to 50 At% iridium is presumed to decompose in a peritectoid reaction into HfIr and $Hf_3Ir_2$ at about 1900°C; X-ray results from arc-melted samples near 48 At% iridium showed small remnants of the HfIr high temperature phase with a predominance of the new phase, $HfIr_{1-x}$, and $Hf_3Ir_2$. By the same token, X-ray films of samples in the region 48 to 50 At.% Ir, equilibrated at lower temperatures, showed

even lesser amounts of the HfIr phase indicating the transformation to be slow and occurring at decreasingly lower temperatures with increasing iridium content.

$HfIr_{1+x}$, the second new phase found in this central portion of the system, is also presumed to decompose in a peritectoid reaction into HfIr and $HfIr_3$ at about 2050°C. In analogy to the experimental evidence for the $HfIr_{1-x}$ phase, lower heat treatment temperatures for samples in the $HfIr_{1+x}$ region yielded decreasing amounts of the HfIr high temperature phase and increasing quantities of the complex pattern of $HfIr_{1+x}$ and $HfIr_3$. Figures 10 through 12 show the metallographic results of some of the alloys in this region.

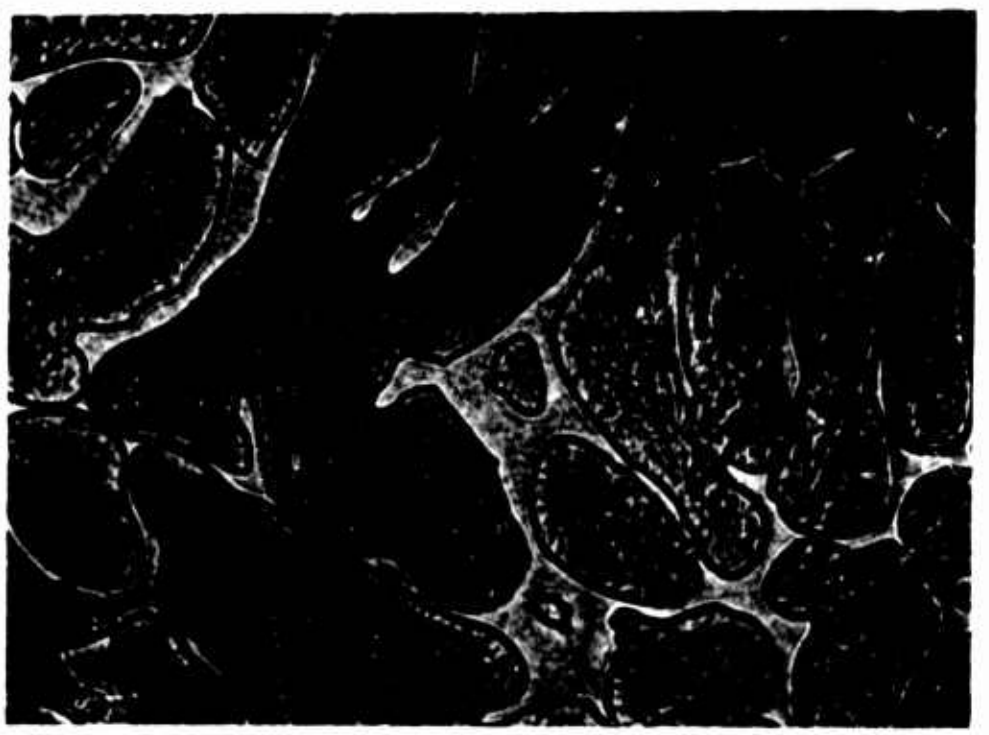

Figure 10. Photomicrograph of a Hf-Ir (52-48) Arc Melted Alloy. Large Grains of Primary HfIr Showing Subsequent Transformation to $HfIr_{1-x}$. Matrix is $Hf_3Ir_2$. X1500

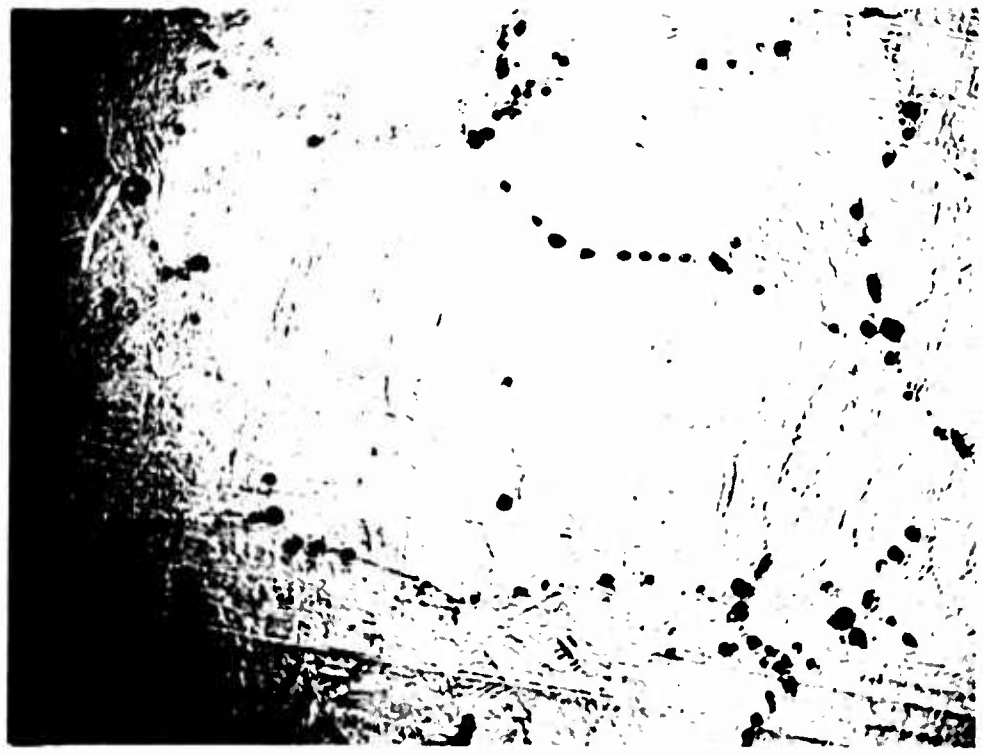

Figure 11. Photomicrograph of a Hf-Ir(51-49) Arc Melted Alloy X1100

Large Grains of Primary HfIr Showing Subsequent Eutectoid Decomposition to $HfIr_{1-x}$ and $HfIr_{1+x}$ close to the Eutectoid Composition.

Figure 12. Photomicrograph of a Hf-Ir (47.5-52.5) Alloy, Initially Melted then Equilibrated and Quenched from 2000°C. X600

Large Grains of Primary HfIr Showing Subsequent Transformation to $HfIr_{1+x}$. Aglomerated HfIr (transformed)-$HfIr_3$ Eutectic in Between Grains.

A eutectic was found to exist between the HfIr phase and the iridium-richest compound, $HfIr_3$. From metallographic inspection as well as from melting behavior, this eutectic was positioned at 63 ± 1 At.% iridium; the eutectic isotherm lies at 2130 ± 15°C. The two photomicrographs shown in Figures 13 and 14 show this eutectic structure. In

Figure 13. Photomicrograph of a Hf-Ir (42-58) Arc Melted X1500 Alloy.

Primary HfIr (transformation not resolved) in a HfIr-$HfIr_3$ Eutectic Matrix.

confirmation of the results published by Dwight and Beck[4], these investigations also revealed a phase at a composition of $HfIr_3$; this intermediate phase has the ordered $Cu_3Au$ type structure with lattice parameters varying between $3.89_5$ and $3.93_1$ Å at 1100°C. The typical superstructure lines in the X-ray patterns of this crystal structure were not observed because the difference in the atomic scattering factors of hafnium and iridium is too small. The $HfIr_3$ has a small homogeneous range about the stoichiometric composition which increases somewhat at higher temperatures. This phase melts congruently and has the highest melting point, 2460 ± 30°C, in the binary hafnium-iridium system.

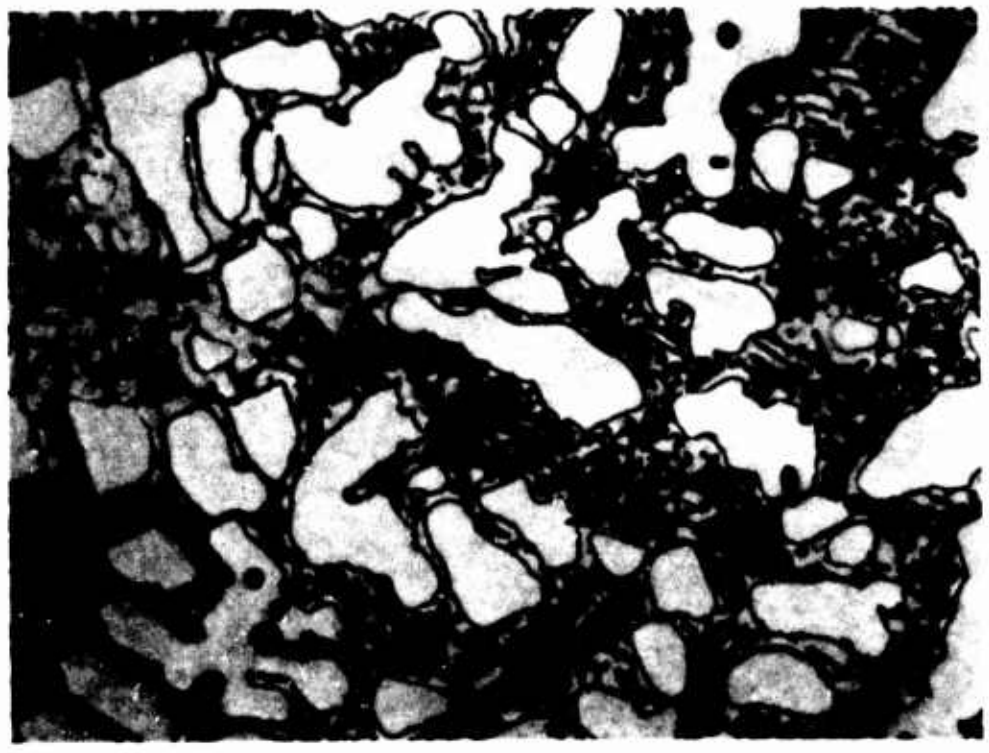

Figure 14. Photomicrograph of a Hf-Ir (33-67) Arc Melted Alloy. X1000

Primary $HfIr_3$ in a $HfIr$-$HfIr_3$ Eutectic Matrix.

Figure 15 shows photomicrograph of a sample in this single phase region. Between the $HfIr_3$ phase and the iridium solid solution there is a eutectic located close to 88 At% iridium; the eutectic temperature, is $2290 \pm 8°C$. The Ir-$HfIr_3$ eutectic appears to be collumnar in nature, and in addition, tends to divorce quite readily. Figure 16 shows the typical eutectic structure observed in this area of the hafnium-iridium binary system.

The solubility of hafnium in iridium was not specifically investigated, although Debye-Scherrer photographs and melting point results indicated only a slight solubility at the most. The solubility of iridium in hafnium, as well as the details of the projection of the $\alpha$-$\beta$ Hf transformation into the binary system were not specifically studied, and hence the $\alpha$-$\beta$ transformation, and the boundary of the hafnium solid solution, are indicated by dashed lines in the proposed constitution diagram.

Figure 15. Photomicrograph of a Hf-Ir (23.5-76.5) Arc Melted Alloy X600

Single Phase $HfIr_3$ (heavily etch pitted). Black Dots are Pores.

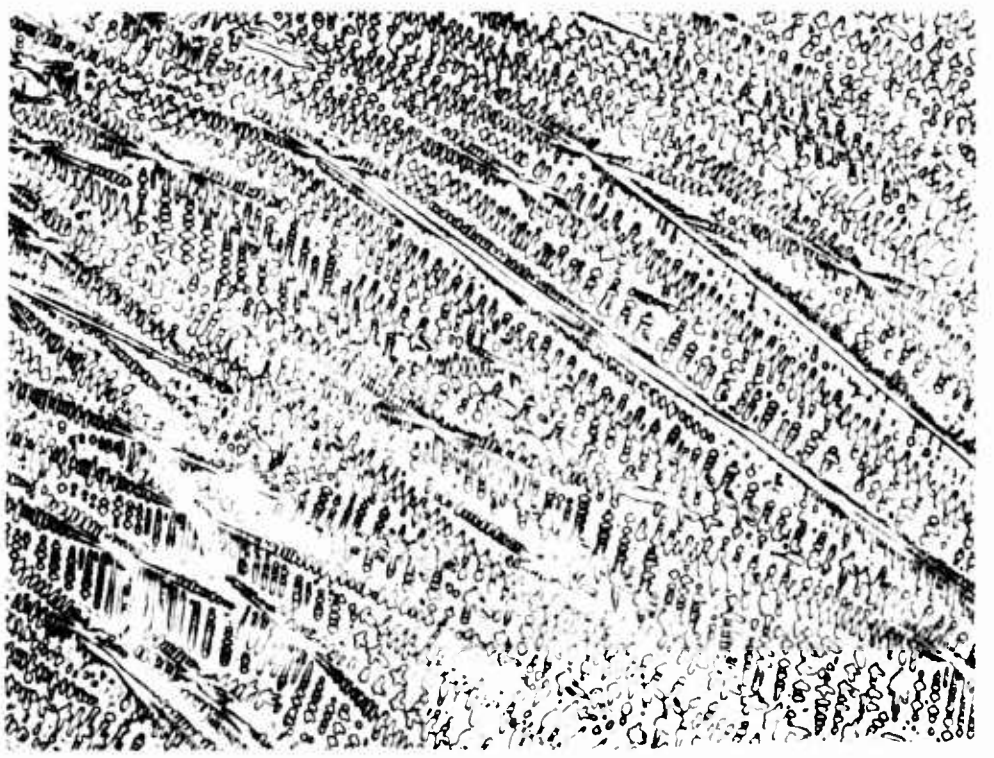

Figure 16. Photomicrograph of a Hf-Ir (15-85) Alloy (Eutectic Portion). X95

$HfIr_3$-Ir Collumnar Eutectic.

It should be noted that the description of the phase equilibria and reactions as well as the semi-schematic enlargement of the central portion of this system are based on the findings of but a few experimental samples, and additional quenching and heat treatment experiments as well as differential thermal analysis runs are necessary for the more accurate determination of the isotherms as well as the location of the temperature dependent boundaries of the coexisting phases.

Figure 17 portrays the melting point data and melting behavior of the hafnium-iridium alloys while Table 6 gives the qualitative X-ray findings of the arc melted and heat treated samples. Figure 18 depicts the hafnium-iridium system constructed from the experimental results.

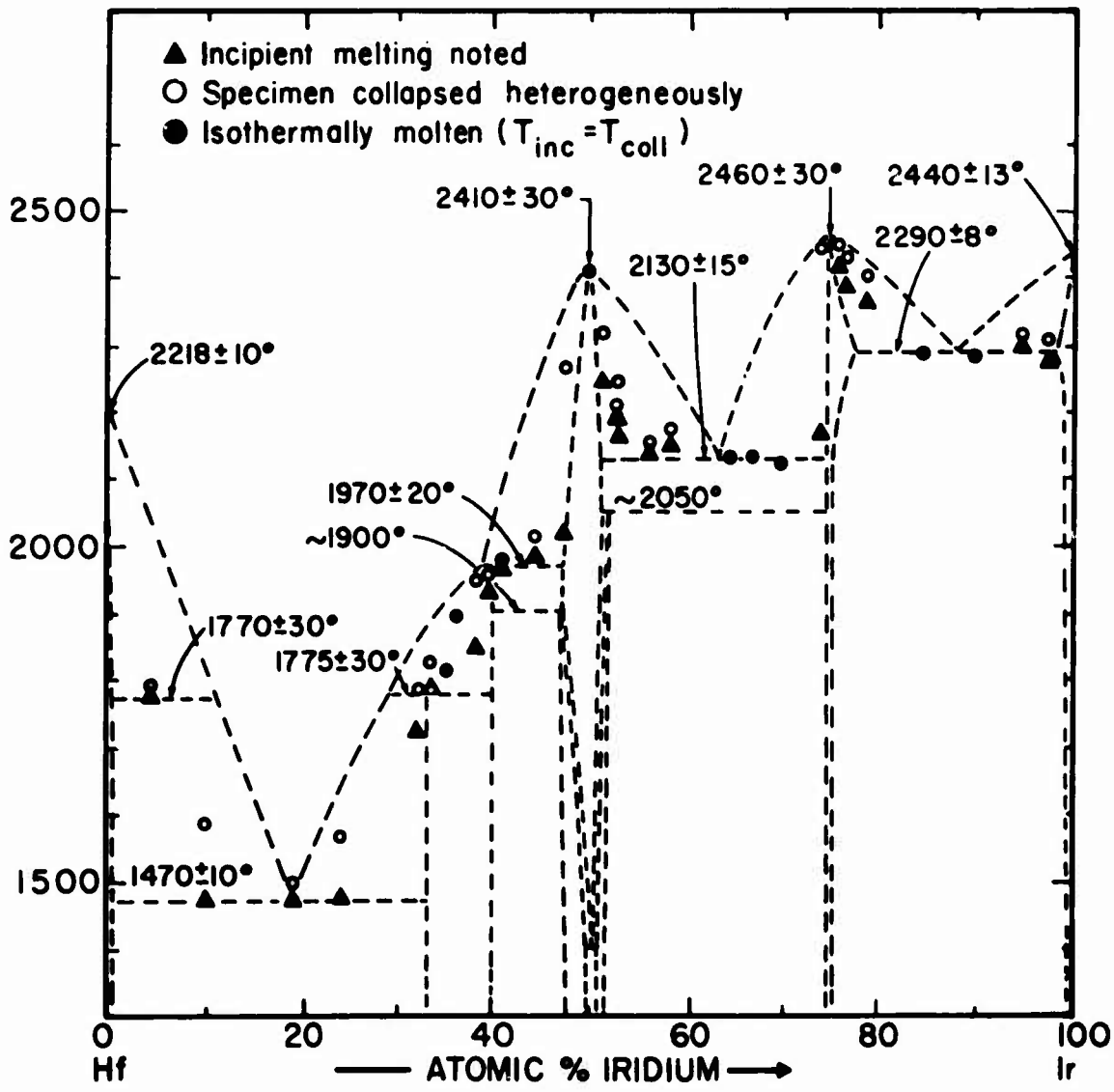


Figure 17. Experimental Melting Point Data in the Hf-Ir System.

Table 6. Qualitative X-ray Analysis of Hafnium-Iridium Alloys

| Nominal Composition At.% Hf | Nominal Composition At.% Ir | Heat Treatment | Phases Present | Remarks |
|---|---|---|---|---|
| 95 | 5 | Arc Melted | α-Hf + $Hf_2Ir$ | |
| 90 | 10 | Arc Melted | α-Hf + $Hf_2Ir$ | |
| 81.5 | 18.5 | Arc Melted | α-Hf + $Hf_2Ir$ | |
| 80 | 20 | Arc Melted | α-Hf + $Hf_2Ir$ | |
| 80 | 20 | Arc Melted + 72 hr/1150° | α-Hf + $Hf_2Ir$ | |
| 75 | 25 | Arc Melted | $Hf_2Ir$ + little α-Hf | |
| 67.5 | 32.5 | Arc Melted | $Hf_2Ir$ + trace $Hf_3Ir_2$ | |
| 67 | 33 | Arc Melted | $Hf_2Ir$ + trace $Hf_3Ir_2$ | |
| 67 | 33 | Arc Melted + 72 hrs/1150° | $Hf_2Ir$ | |
| 66.5 | 33.5 | Arc Melted | $Hf_2Ir$ + trace $Hf_3Ir_2$ | |
| 65 | 35 | Arc Melted | $Hf_2Ir$ + $Hf_3Ir_2$ | |
| 63.3 | 36.7 | Arc Melted | $Hf_2Ir$ + $Hf_3Ir_2$ | |
| 61.5 | 38.5 | Arc Melted | $Hf_3Ir_2$ + trace $Hf_2Ir$ | |
| 60 | 40 | Arc Melted | $Hf_3Ir_2$ + trace HfIr | |
| 60 | 40 | Arc Melted + 72 hrs/1150° | $Hf_3Ir_2$ + trace HfIr | HfIr trans. incomp. |
| 59 | 41 | Arc Melted | $Hf_3Ir_2$ + trace HfIr | |
| 55.5 | 44.5 | Arc Melted | $Hf_3Ir_2$ + little HfIr | |
| 52 | 48 | Arc Melted | HfIr + little $Hf_3Ir_2$ | HfIr transfmg. |
| 52 | 48 | Arc Melted + 63 hrs/1460° | $HfIr_{1-x}$ + HfIr | HfIr transfmg. |
| 52 | 48 | Arc Melted + 1/2 hr powder anneal/1100° | $HfIr_{1-x}$ + HfIr | HfIr trans. incomp. |
| 51 | 49 | Quenched from 2256° | $HfIr_{1-x}$ + HfIr | HfIr transfmg. |
| 50 | 50 | Arc Melted | HfIr | |
| 50 | 50 | Arc Melted + 72 hrs/1150° | HfIr + $HfIr_{1-x}$ + $HfIr_{1+x}$ | trans. incomp. |
| 50 | 50 | Arc Melted + 63 hrs/1460° | HrIr + ? | extrem. diffuse |
| 50 | 50 | Arc Melted + 63 hrs/1460° + powder anneal/1100° | HfIr + $HfIr_{1-x}$ | trans. incomp. |
| 48.8 | 51.2 | Arc Melted | HfIr | extrem. diffuse |

Table 6 (continued)

| Nominal Composition At.% Hf | Ir | Heat Treatment | Phases Present | Remarks |
|---|---|---|---|---|
| 48.8 | 51.2 | Arc Melted + 63 hrs/1460° | $HfIr_{1+x}$ + tr. $HfIr_3$ + tr HfIr | trans. incomp. |
| 47.5 | 52.5 | Arc Melted | HfIr + tr $HfIr_3$ | extrem. diffuse |
| 47.5 | 52.5 | Equil. at 2000° and Quench | $HfIr_{1+x}$ + $HfIr_3$ | |
| 47.5 | 52.5 | Arc Melted + 63 hrs/1460° | HfIr+$HfIr_3$+$HfIr_{1+x}$ | trans. incomp. |
| 44 | 56 | Arc Melted | Hf + $HfIr_3$ | |
| 44 | 56 | Arc Melted + 63 hrs/1460° | HfIr+$HfIr_3$ +little $HfIr_{1+x}$ | trans. incomp. |
| 42 | 58 | Arc Melted | HfIr + $HfIr_3$ | |
| 42 | 58 | Arc Melted + 63 hrs/1460° | HfIr+$HfIr_3$ + little $HfIr_{1+x}$ | trans. incomp. |
| 42 | 58 | Arc Melted + 1/2 hr powder anneal/1100° | $HfIr_3$+$HfIr_{1+x}$ + tr HfIr | trans. incomp. |
| 40 | 60 | Arc Melted | $HfIr_3$+HfIr+$HfIr_{1+x}$ | trans. incomp. |
| 40 | 60 | Arc Melted + 72 hrs/1150° | $HfIr_3$+HfIr + $HfIr_{1+x}$ | trans. incomp. |
| 35 | 65 | Arc Melted | $HfIr_3$ + tr HfIr | |
| 35 | 65 | Arc Melted + 63 hrs/1460° | $HfIr_3$ + tr HfIr | |
| 35 | 65 | Arc Melted + 1/2 hr powder anneal/1100° | $HfIr_3$ + tr $HfIr_{1+x}$ | |
| 33 | 67 | Arc Melted | $HfIr_3$ + tr HfIr | |
| 30 | 70 | Arc Melted | $HrIr_3$ + tr HfIr | |
| 26 | 74 | Arc Melted | $HfIr_3$ | |
| 25 | 75 | Arc Melted | $HfIr_3$ | |
| 25 | 75 | Arc Melted + 72 hrs/1150° | $HfIr_3$ | |
| 23.5 | 76.5 | Arc Melted | $HfIr_3$ | |
| 23.5 | 76.7 | Arc Melted | $HfIr_3$ | |
| 21 | 79 | Arc Melted | $HfIr_3$ + Ir | |
| 15 | 85 | Arc Melted | $HfIr_3$ + Ir | |
| 15 | 85 | Arc Melted + 72 hrs/1150° | $HfIr_3$ + Ir | |
| 10 | 90 | Arc Melted | $HfIr_3$ + Ir | |
| 6 | 94 | Arc Melted | Ir + tr $HfIr_3$ | |
| 2.5 | 97.5 | Arc Melted | Ir + barest tr $HfIr_3$ | |

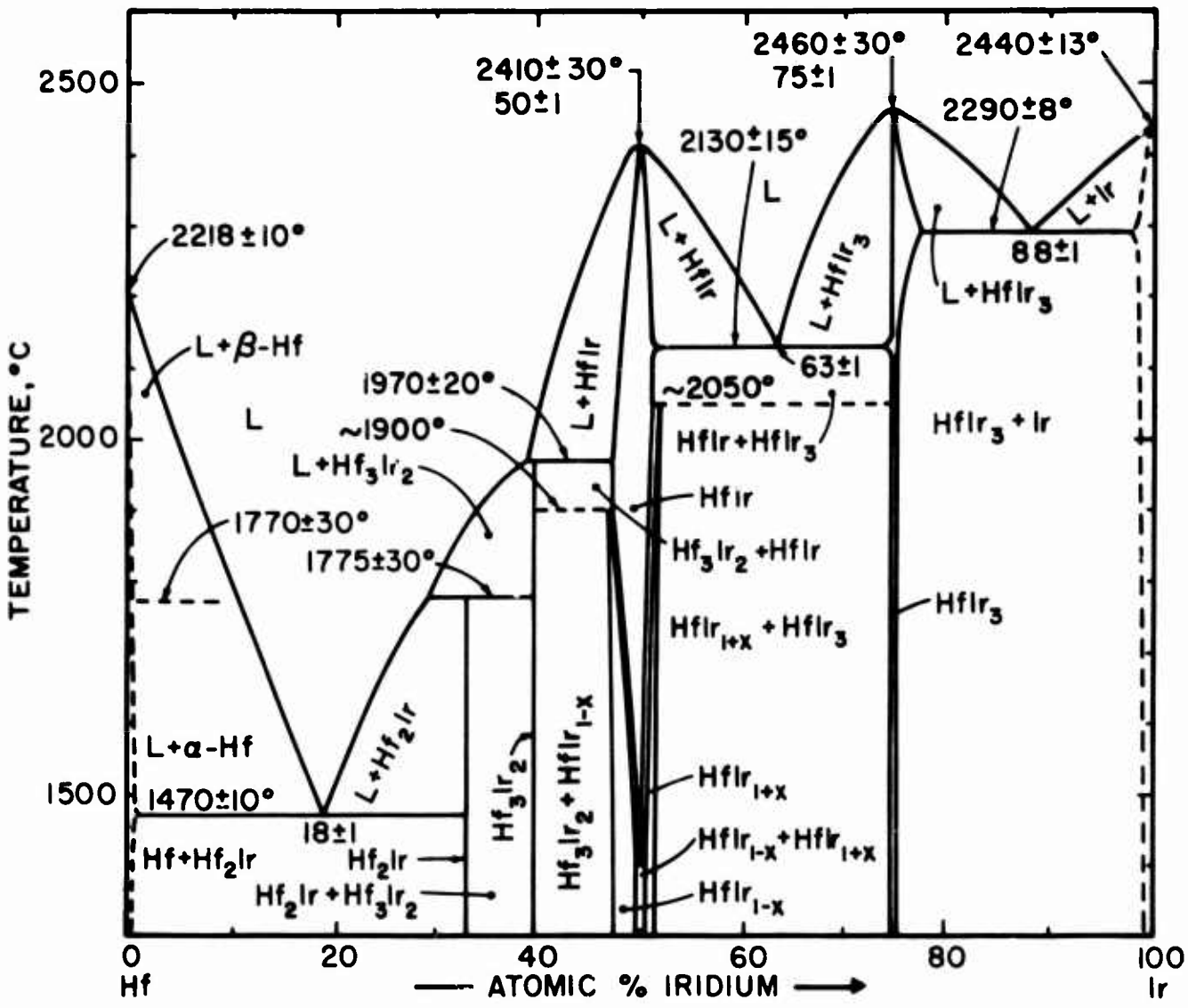


Figure 18. The Hafnium-Iridium System

## B. IRIDIUM-BORON

Figure 19 shows the composition as well as the type of melting observed with the Pirani melting point specimens; Table 7 lists the melting point results of the individual samples.

The melting temperatures of the samples in the region Ir-$Ir_3B_2$ showed that a eutectic isotherm is present at 1250 ± 6°C. With the aid of metallography, this eutectic between iridium and $Ir_3B_2$ was placed at

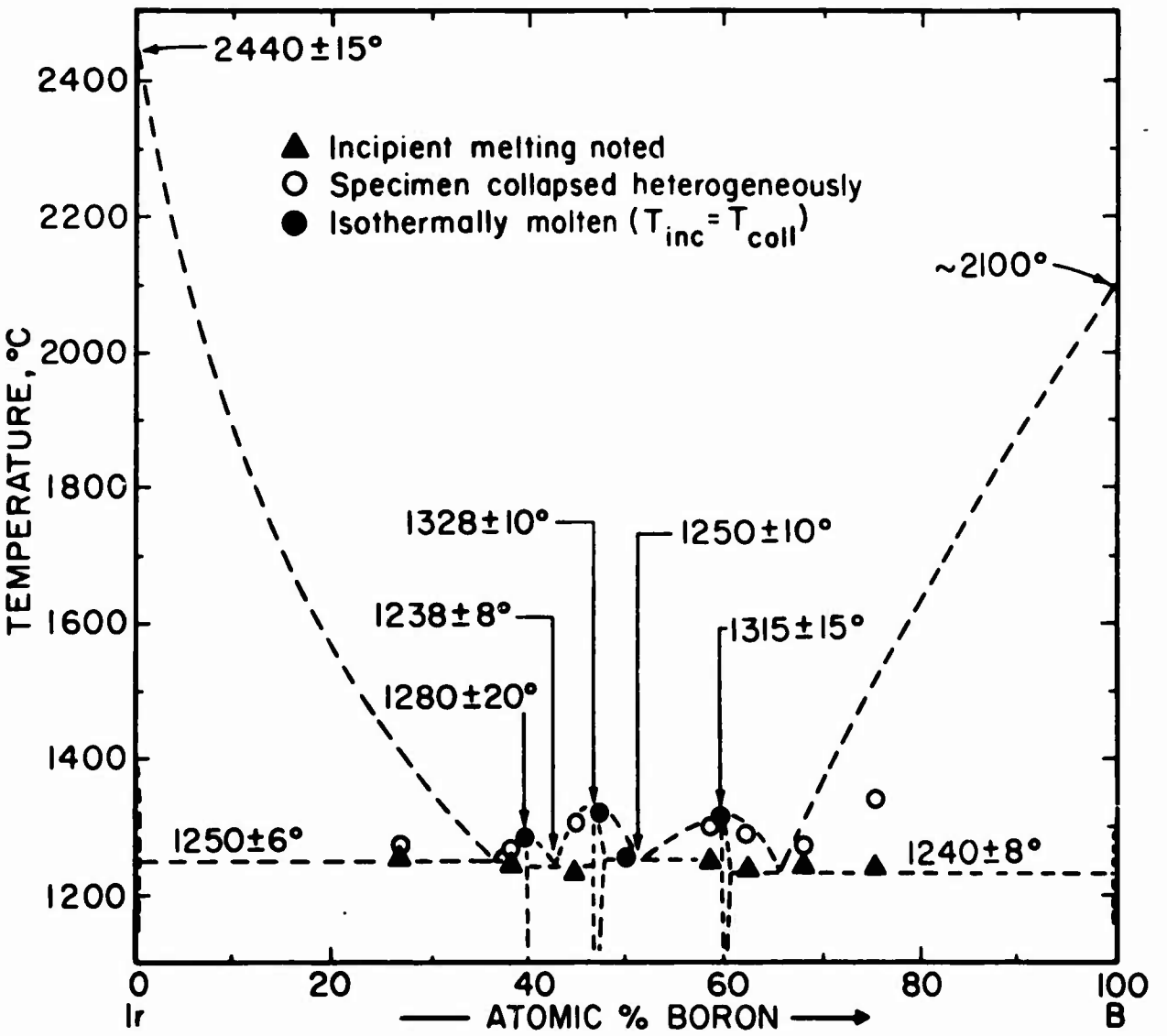


**Figure 19. Sample Location and Observed Melting Behavior in the Iridium-Boron System.**

Table 7. Observed Melting Behavior and Qualitative X-ray Analysis of Iridium-Boron Alloys

| Sample Composition Nominal At.% | | Melting Temperatures °Centigrade | | Qualitative X-ray Findings |
|---|---|---|---|---|
| Iridium | Boron | Incipient | Collapse | Phases Present |
| 75 | 25 | 1251 | 1256 | Iridium + $Ir_3B_2$ |
| 62 | 38 | 1247 | 1253 | $Ir_3B_2$ + trace Iridium |
| 60 | 40 | 1280 | 1280 | $Ir_3B_2$ + trace Iridium |
| 55 | 45 | 1240 | 1308 | $Ir_3B_2$ + $IrB_{0.89}$ |
| 52.5 | 47.5 | 1328 | 1328 | $IrB_{0.89}$ |
| 49 | 51 | 1251 | 1251 | $IrB_{0.89}$ + $IrB_{1.50}$ |
| 41 | 59 | 1255 | 1295 | $IrB_{1.50}$ + little $IrB_{0.89}$ |
| 40 | 60 | 1315 | 1315 | $IrB_{1.50}$ |
| 37.5 | 62.5 | 1237 | 1287 | $IrB_{1.50}$ + trace B |
| 33.3 | 66.7 | 1246 | 1251 | $IrB_{1.50}$ + little B |
| 25 | 75 | 1241 | 1330 | $IrB_{1.50}$ + little B |

36 $\pm$ 1 At.% boron. Figures 20 and 21 show the photomicrographs of alloys in this region. The phase lying near 40 At.% B had been observed earlier[5] in samples not post-experimentally analyzed. The existence of this phase at a composition closely corresponding to the formula $Ir_3B_2$ may be regarded as confirmed, although the crystal structure has not been elucidated as yet. Table 8 presents the measured lines of the powder diffraction pattern of the phase quite close to the composition $Ir_3B_2$.

Figure 20. Photomicrograph of an Ir-B (75-25) Arc Melted Alloy. X680

Primary Iridium Grains (White) in $Ir_3B_2$ Matrix.

Figure 21. Photomicrograph of an Ir-B (Anal: 61.3-38.7) Arc Melted Alloy. X160

Elongated Primary $Ir_3B_2$ Grains (Grey-White) in Ir-$Ir_3B_2$ Eutectic Matrix.

Table 8. Diffraction Pattern of the Ir-B Phase Near 40 At.% B Cu $K_a$ Radiation

| $Sin^2\theta$ | Estimated Intensity | Remarks |
|---|---|---|
| .07432 | 3 | |
| .09974 | 5 | |
| .17448 | 7 dif | |
| .30079 | 2+ | |
| .37513 | 3 | |
| .39758 | 3+ | |
| .47503 | 2 | |
| .59678 | 2 dif | |
| .66657 | 1- | |
| .69889 | 4 dif | |
| .76776 | 10 | Coincidence with Ir line |
| .89826 | 1+ dif | |
| .96955 | 10 | Coincidence with Ir line |

The $Ir_3B_2$ phase melts congruently at 1270 ± 20°C, a temperature not too much higher than the two neighboring eutectic isotherms.

Melting point measurements, as well as the type of melting observed indicate that a eutectic occurs between the two congruently melting compounds $Ir_3B_2$ and $IrB_{0.89}$ at 1238 ± 8°C although no metallographic pictures are available showing this eutectic.

The phase observed near 50 At.% boron has the crystal structure corresponding to the phase described by Arronson et al.[7,8] at a composition of $IrB_{\sim 1.1}$; this crystal structure is isomorphic with the $ThSi_2$ tetragonal structure. Attempts were made to index the Debye-Scherrer pattern of this phase according to the hexagonal C-32 structure as suggested by

a Russian[9] publication; however, the results were not satisfactory, but excellent agreement was found using the structure ($ThSi_2$-Type) proposed by Aronsson[7,8]. The lattice parameters determined were: $a = 2.80_7$ and $c = 10.25$ Å. The composition of this phase is now designated as $IrB_{0.89}$ on the basis of analyzed metallographic samples and Debye-Scherrer X-ray patterns of alloys in this vicinity.

Figure 22 shows a photomicrograph of an Ir-B alloy whose analyzed boron content was 44.0 At.%.

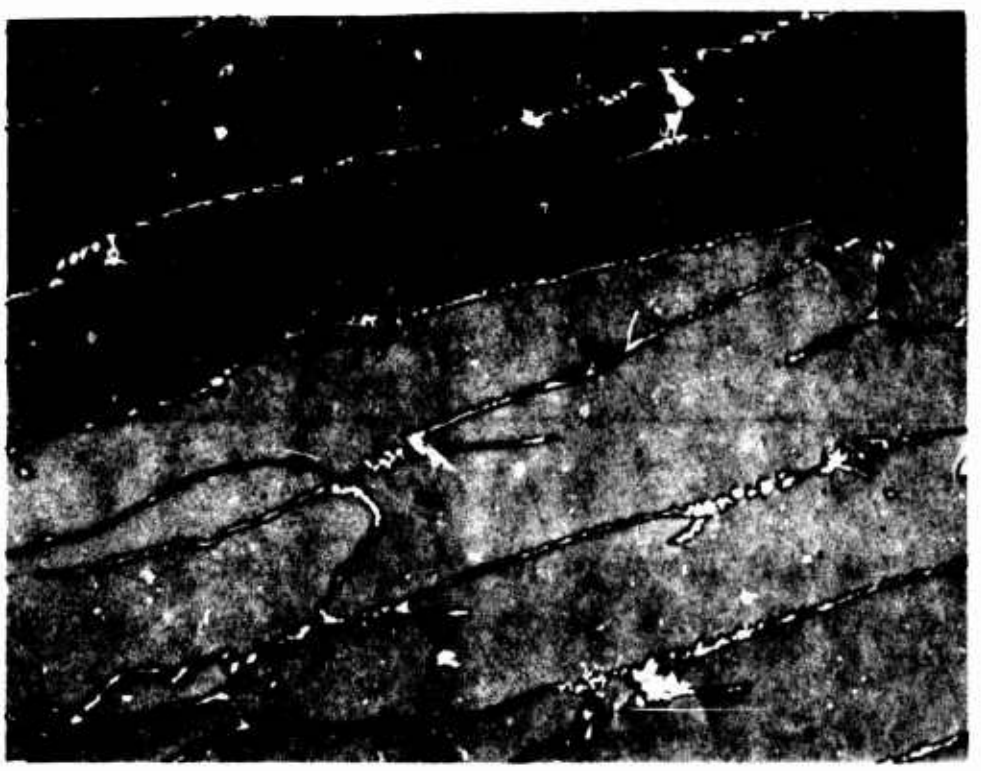

Figure 22. Photomicrograph of an Ir-B (Anal: 56.0-44.0) Arc Melted Alloy. X600

$IrB_{0.89}$ Grains with Small Amounts of $Ir_3B_2$ on Grain Boundaries.

A small range of homogeneity, centered around 47 At.% boron, is assigned to the $IrB_{0.89}$ phase on the basis of qualitative X-ray phase analysis, lattice parameter variations, and analyzed metallographic samples. The changes in lattice parameters of the $IrB_{0.89}$ phase are shown in Table 9 and

indicate that the homogeneous range of the $IrB_{0.89}$ phase increases slightly at temperatures above 1000°C.

Table 9. Lattice Parameter Variations of the $IrB_{0.89}$ Phase.

| Composition At.% | | Heat Treatment | Lattice Parameters in Angstroms | |
|---|---|---|---|---|
| Ir | B | | a | c |
| 55 | 44(anal) | Arc Melted + 64 hrs/1000°C | $2.80_7$ | $10.25_0$ |
| 56 | 44(anal) | Arc Melted | $2.80_8$ | $10.25_9$ |
| 49.8 | 50.2(anal) | Arc Melted + 64 hrs/1000°C | $2.80_7$ | $10.24_6$ |
| 49.8 | 50.2(anal) | Arc Melted | $2.81_1$ | $10.24_8$ |
| 37.5 | 62.5(nom) | Quenched from 1290°C | $2.80_7$ | $10.25_2$ |
| 52.5 | 47.5(nom) | Arc Melted Quenched from 1330°C | $2.80_6$ | $10.25_3$ |

This phase was found to melt congruently at 1328 ± 10°C at a composition of about 47 At.% boron.

Analyzed metallographic specimens and melting point data showed the existence of a eutectic between the phases $IrB_{0.89}$ and $IrB_{1.50}$ at 50 ± 1 At.% boron; the eutectic temperature was measured at 1250 ± 10°C. Figure 23 shows the eutectic structure obtained from a sample with an analyzed boron content of 50.2 At.%.

Figure 23. Photomicrograph of an Ir-B(Anal: 49.8-50.2) Arc Melted Alloy. X325

$IrB_{0.89}$-$IrB_{1.50}$ Eutectic.

The third and last phase observed in these investigations of the iridium boron system is apparently one of the phases reported by Buddery and Welch[5]. This phase was located near the composition $IrB_2$, but the exact composition was designated as being uncertain[5]. The intermediate crystal structure is certainly not the phase described by Russian authors[9] in the range 50-67 At.% boron with the hexagonal C-32 structure, for the Debye-Scherrer powder photograph of this crystal structure is far more complex than the pattern presented by the C-32 type.

Attempts at indexing this powder pattern were unsuccessful, and it would seem as though single crystal studies will be necessary to characterize this crystal structure. Table 10 shows the Debye-Scherrer pattern observed for this phase near 60 At.% boron.

Table 10. Diffraction Pattern of the Ir-B Phase Near 60 At.% Boron. $CrK_\alpha$ Radiation

| $Sin^2\theta$ | Estimated Intensity | Remarks | $Sin^2\theta$ | Estimated Intensity | Remarks |
|---|---|---|---|---|---|
| .08383 | 2 | | .57632 | 1 | |
| .14142 | 3 | | .59181 | 1- | |
| .18575 | 4+ | | .60617 | 3 | |
| .19080 | 6- | Coincidence | .62806 | 1 | Diffuse |
| .20385 | 8- | | .73735 | 8 | Coincidence |
| .22856 | 2 | | .75901 | 9 | |
| .29999 | 4+ | Coincidence, diffuse | .78665 | 1+ | |
| .32473 | 2 | | .80007 | 2 | |
| .35968 | 1 | | .80258 | 8+ | Coincidence, diffuse |
| .37110 | 4 | | .88714 | 10 | Diffuse |
| .41112 | 4 | | .92207 | 3 | |
| .46825 | 1+ | | .93798 | 4 | |
| .48552 | 8+ | Coincidence | .95174 | 1+ | Diffuse |
| .55851 | 1 | | .97138 | 6+ | |

Metallographic evidence, supported by chemica' analysis and qualitative X-ray phase analysis indicate that the intermediate phase in the region of 50-67 At.% boron is located quite close to 60 At.% boron; this congruently melting compound was found to meli at 1315 $\pm$ 15°C. Figure 24 shows an almost single phased alloy near 60 At.% boron, while Figure 25 shows this same phase with some amount of free boron at 67 At.% boron.

Although no metallographic evidence was obtained to support the supposition that a eutectic must exist between boron and the $IrB_{1.50}$ phase, the melting behavior and melting point measurements strongly indicate the presence of a eutectic; on the basis of the information available, this eutectic is estimated at about 66 At.% boron; the eutectic temperature is 1240 $\pm$ 8°C.

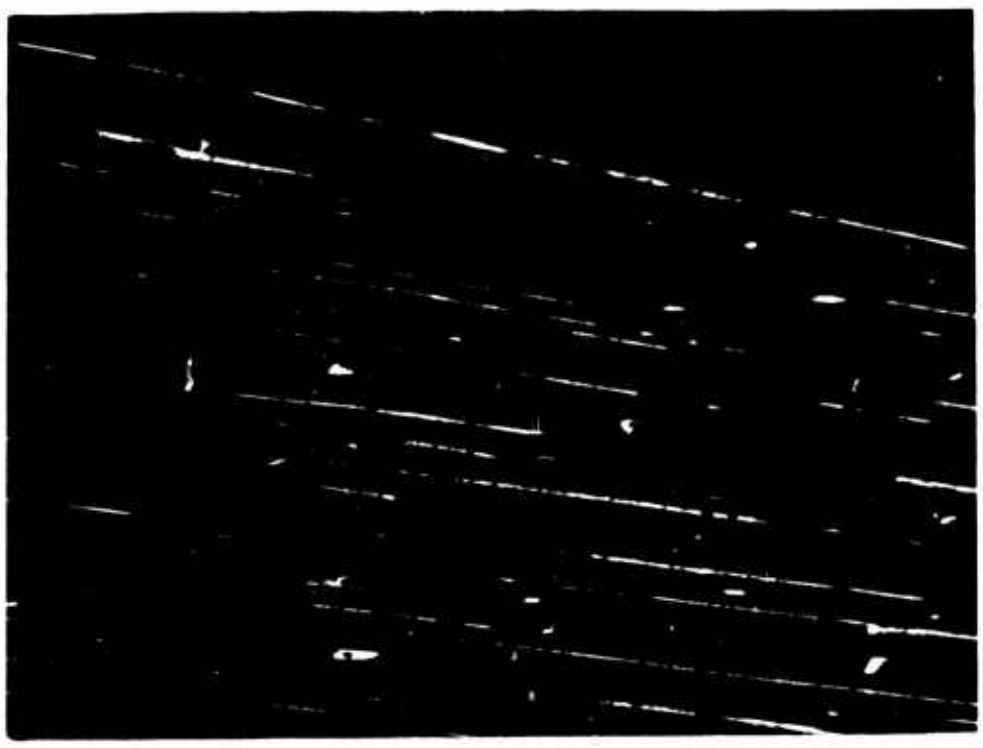

Figure 24. Photomicrograph of an Ir-B (Anal: 39.2-60.8) Arc Melted Alloy. X275

$IrB_{1.50}$ Phase with Small Amounts of $IrB_{0.89}$ on the Grain Boundaries.

Figure 25. Photomicrograph of an Ir-B (33-67) Arc Melted Alloy. X400

Large and Small Boron Inclusions (White and Black) in a Matrix of $IrB_{1.50}$.

Figure 26 shows a two phased Ir-B alloy at 75 At.% boron. The eutectics of borides with boron are, in general, quite difficult to observe metallographically; however, traces of the typical worm-like boron-boride eutectic are visible in the $IrB_{1.50}$ grains.

Figure 27 depicts the phase diagram of the iridium-boron system constructed with the data obtained in these investigations. The solubility of iridium in boron is assumed to be quite small, and the solubility of boron is indicated to be minimal as stated by Aronsson[7].

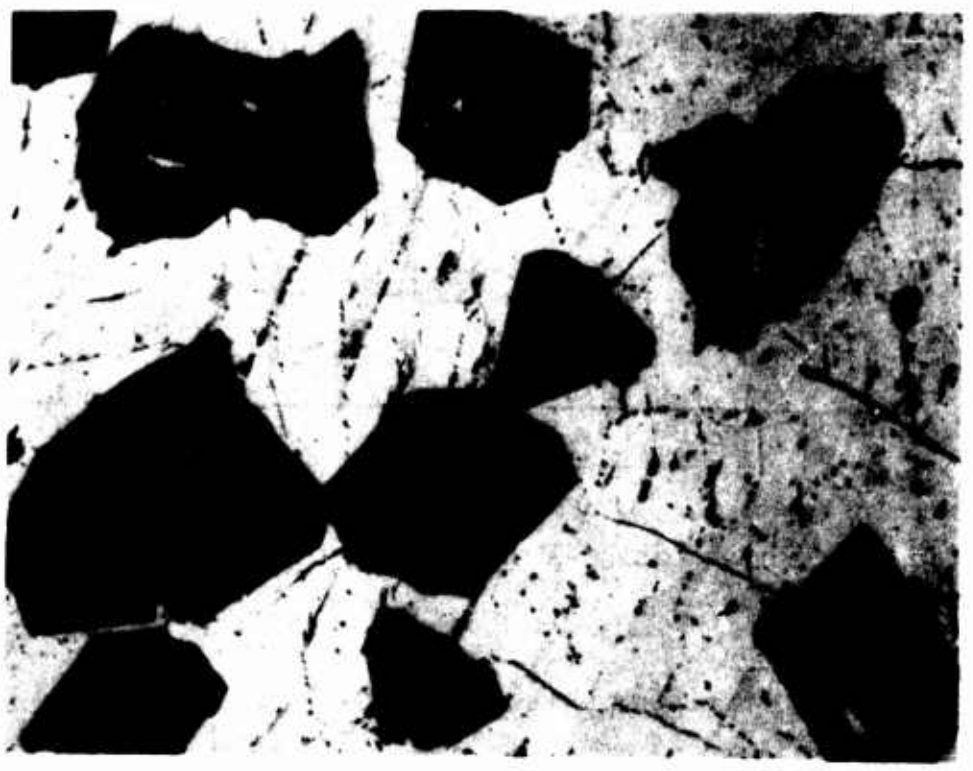

Figure 26. Photomicrograph of an Ir-B (25-75) Arc Melted Alloy. X440

Large Black Grains of Primary Crystallized Boron in a $IrB_{1.50}$ + Boron Eutectic Matrix.

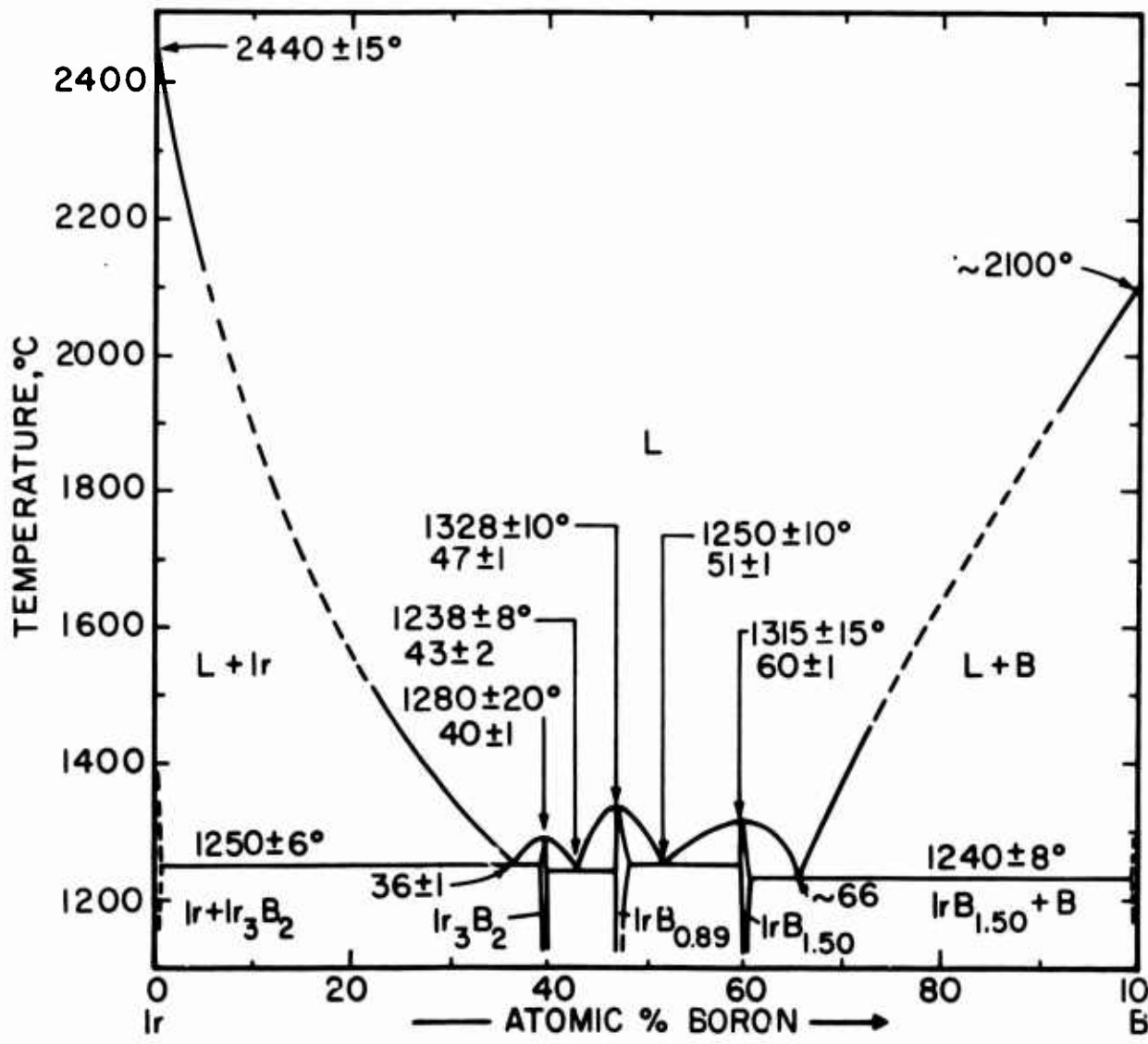


Figure 27. The Iridium-Boron System.

## C. HAFNIUM-IRIDIUM-BORON

The fifty-four samples, most of which received heat treatments at 1100°C, were used to establish an isothermal section of the hafnium-iridium-boron system at 1100°C; this rather low temperature was a forced choice because the melting points of the binary Ir-B system, except for the elements themselves, are quite low. The phase equilibria in the ternary system at 1100°C was established primarily on the basis of the evaluation of the Debye-Scherrer X-ray patterns.

The most stable binary phase, $HfB_2$, forms equilibria with almost all of the Hf-Ir binary phases and most of the ternary phases present; in addition, the $HfIr_3(B)$ solid solution also forms two-phase equilibria with the majority of the iridium-rich phases, both ternary and binary.

Figure 28 shows the compositional location and qualitative X-ray findings of the many ternary samples investigated at 1100°C; Table 11 lists these qualitative X-ray findings.

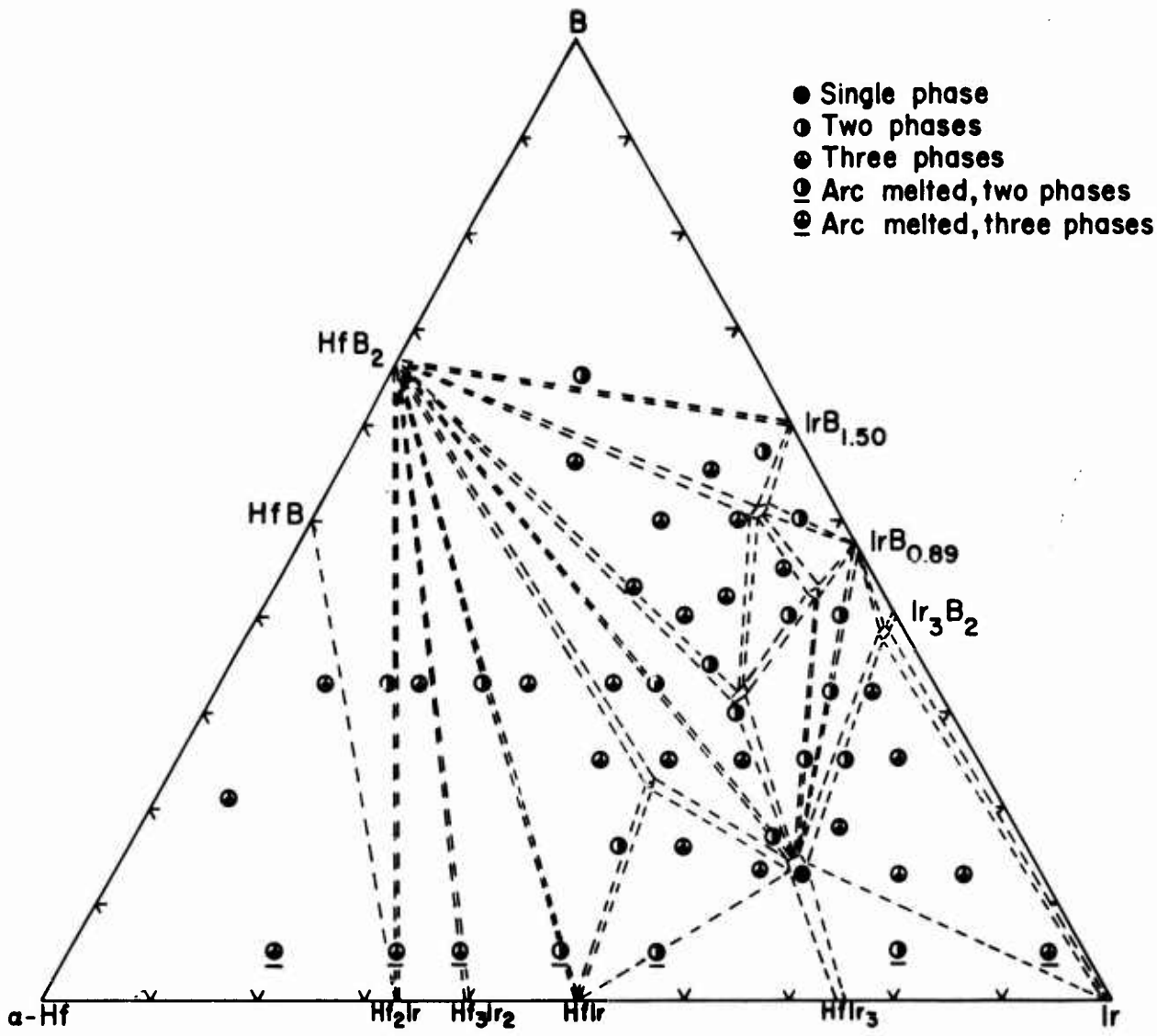


Figure 28. Compositional Location and Qualitative X-ray Analysis of Ternary Hf-Ir-B Samples at 1100°C.

Table 11. Qualitative X-ray Results of Hf-Ir-B Ternary Samples.

| Nominal Composition At.% | | | Phases Present |
|---|---|---|---|
| Hf | Ir | B | |
| 7 | 80 | 13 | Ir + $HfIr_3$(B) + $T_3$ |
| 13 | 74 | 13 | Ir + $HfIr_3$(B) + $T_3$ |
| 22 | 65 | 13 | $HfIr_3$(B) |
| 27 | 60 | 13 | $HfIr_3$(B) + little $T_4$ + little HfIr |
| 32 | 52 | 16 | $HfIr_3$(B) + $T_4$ + HfIr |
| 38 | 46 | 16 | $T_4$ + HfIr |
| 23 | 60 | 17 | $HfIr_3$(B) + tr $HfB_2$ |
| 16 | 66 | 18 | $HfIr_3$(B) + little Ir + little $T_3$ |
| 71 | 7 | 22 | $HfB_2$ + α-Hf + $Hf_2Ir$ |
| 7 | 68 | 25 | $HfIr_3$(B) + $T_3$ + Ir |
| 12 | 63 | 25 | $T_3$ + $HfIr_3$(B) |
| 16 | 59 | 25 | $HfIr_3$(B) + $T_5$ |
| 22 | 53 | 25 | $HfIr_3$(B) + $T_1$ + trace $HfB_2$ |
| 29 | 46 | 25 | $T_4$ + $HfIr_3$(B) + little $HfB_2$ |
| 35 | 40 | 25 | $T_4$ + little HfIr + little $HfB_2$ |
| 20 | 50 | 30 | $T_1$ + trace $HfIr_3$(B) |
| 6 | 62 | 32 | $T_3$ + little $HfIr_3$(B) + tr Ir |
| 10 | 58 | 32 | $HfIr_3$(B) + $IrB_{0.89}$ |
| 26 | 41 | 33 | $HfIr_3$(B) + $HfB_2$ |
| 30 | 37 | 33 | $HfB_2$ + $T_4$ + $HfIr_3$(B) |
| 38 | 29 | 33 | $HfB_2$ + little HfIr + $T_4$ |
| 42 | 25 | 33 | HfIr + $HfB_2$ |
| 48 | 19 | 33 | $HfB_2$ + little $Hf_3Ir_2$ + little $Hf_2Ir$ |
| 51 | 16 | 33 | $HfB_2$ + $Hf_2Ir$ |
| 57 | 10 | 33 | $HfB_2$ + $Hf_2Ir$ + little α-Hf |
| 20 | 45 | 35 | $T_1$ + $HfB_2$ |
| 5 | 55 | 40 | $IrB_{0.89}$ + $HfIr_3$(B) |

Table 11. Qualitative X-ray Results of Hf-Ir-B Ternary Samples.

| Nominal Composition At.% | | | Phases Present |
|---|---|---|---|
| Hf | Ir | B | |
| 10 | 50 | 40 | $T_5 + T_1$ |
| 20 | 40 | 40 | $T_1 + HfB_2$ + little $T_2$ |
| 15 | 43 | 42 | $T_1 + HfB_2 + T_2$ |
| 23 | 34 | 43 | $HfB_2 + T_1$ + little $T_2$ |
| 8 | 47 | 45 | $T_2 + T_5$ + little $T_1$ |
| 4 | 46 | 50 | $IrB_{0.89} + T_2$ |
| 10 | 40 | 50 | $T_2$ + trace $HfB_2$ + trace $T_1$ |
| 17 | 33 | 50 | $HfB_2 + T_1 + T_2$ |
| 10 | 35 | 55 | $T_2 + IrB_{1.50} + HfB_2$ |
| 22 | 22 | 56 | $HfB_2 + T_2 + T_1$ |
| 4 | 39 | 57 | $IrB_{1.50} + T_2$ |
| 17 | 18 | 65 | $HfB_2 + IrB_{1.50}$ |
| Arc Melted Samples: | | | |
| 3 | 92 | 5 | Ir + trace HfIr (B) + trace $T_3$ |
| 17 | 78 | 5 | $HfIr_3$(B) + Ir |
| 40 | 55 | 5 | HfIr + $HfIr_3$(B) |
| 49 | 46 | 5 | HfIr + trace $HfB_2$ |
| 58 | 37 | 5 | $Hf_3Ir_2$ + trace $Hf_2Ir$ + trace $HfB_2$ |
| 64 | 31 | 5 | $Hf_2Ir$ + trace $Hf_3Ir_2$ + trace $HfB_2$ |
| 76 | 19 | 5 | α-Hf + trace $HfB_2$ + $Hf_2Ir$ |

There are no less than five ternary phases in the hafnium-iridium-boron system; their compositions are: $Hf_{.32}Ir_{.46}B_{.22}(T_4)$, $Hf_{.19}Ir_{.49}B_{.32}(T_1)$, $Hf_{.07}Ir_{.51}B_{.42}(T_5)$, $Hf_{.07}Ir_{.42}B_{.51}(T_2)$, and $Hf_{.02}Ir_{.60}B_{.38}(T_3)$. All of these ternary phases have complicated Debye-Scherrer powder diagrams except the $Hf_{.19}Ir_{.49}B_{.32}(T_1)$ phase which appears to be a distorted modification of the face-centered cubic $HfIr_3(B)$ lattice. It seems probable that a tetragonal indexing of this pattern is possible, but as yet no completely satisfactory results have been obtained. Table 12 shows the measured lines of this binary phase's diffraction pattern.

Table 12. Diffraction Pattern of the Ternary Phase $Hf_{.19}Ir_{.49}B_{.32}$ ($T_1$) $CuK_\alpha$ Radiation

| $Sin^2\theta$ | Estimated Intensity | $Sin^2\theta$ | Estimated Intensity |
|---|---|---|---|
| .15103 | 7- | .70766 | 1+ |
| .16272 | 6- | .71997 | 4 dif |
| .28081 | 2 | .74042 | 6 |
| .30127 | 5 | .75211 | 1-dif |
| .31319 | 6 | .76437 | 5 |
| .38447 | 3+ | .78277 | 3-dif |
| .41714 | 7 | .79811 | 6 |
| .43993 | 6 | .84291 | 2+ |
| .46025 | 6 dif | .85991 | 1 dif |
| .46790 | | .88043$a_1$ | 5 |
| .60242 | 2 | .91226$a_1$ | 7+ |
| .64752 | 3 | .94676$a_1$ | 9- |
| .69489 | 2- | .95189$a_1+a_2$ | ~5 |

Because of the expensive nature of the sample material involved, a considerable number of additional samples would have been necessary to precisely locate and obtain single phase X-ray films of the ternary

phases $Hf_{.02}Ir_{.60}B_{.38}$, and $Hf_{.07}Ir_{.51}B_{.42}$; however, since quite a number of ternary samples were laid in the vicinity of these two phases, a more than necessary amount of information was obtained, and the compositional locations of these ternary phases were able to be established with sufficient accuracy.

Tables 13 and 14 present the measured diffraction patterns of the other ternary phases which were able to be measured without excessive suppression and interference from neighboring patterns appearing on the Debye-Scherrer powder photographs. These complex patterns have not yet been elucidated.

Table 13. Diffraction Pattern of the Ternary Phase $Hf_{.07}Ir_{.42}B_{.51}(T_2)$ $CrK_a$ Radiation

| $Sin^2\theta$ | Estimated Intensity | $Sin^2\theta$ | Estimated Intensity |
|---|---|---|---|
| .12333 | 3 | .58510 | 3 |
| .20133 | 6 | .64752 | 5 |
| .21594 | 3 | .69247 | 8+ |
| .23238 | 6+ | .71036 | 7 |
| .27799 | 4 | .73827 | 1 dif |
| .32441 | 4- | .75632 | 1 dif |
| .36975 | 2 | .76850 | 2 |
| .40049 | 6- | .80161 | 3 |
| .43335 | 4 | .83209 | 9 |
| .47854 | 2 | .86124 | 4 |
| .48446 | 1+ | .87667 | 10 |
| .50908 | 5 | .93798 | 5 |
| .55625 | 3+ | .96840 | 5+ |

Table 14. Diffraction Pattern of $Hf_{.32}Ir_{.46}B_{.22}$ ($T_4$) Ternary Phase $CrK_\alpha$ Radiation

| $Sin^2\theta$ | Estimated Intensity | $Sin^2\theta$ | Estimated Intensity |
|---|---|---|---|
| .14992 | 1 | .64117 | 4 |
| .19659 | 6 | .67199 | 5+ |
| .24443 | 5 | .69022 | 3 |
| .26127 | 5 | .70193 | 1- |
| .27347 | 6 | .72044 | 1- |
| .30785 | 4 | .73257 | 2 |
| .31952 | 4- | .73735 | 5 |
| .36571 | 1+ | .74727 | 5 |
| .42420 | 1 | .76600 | 4 |
| .44548 | 1- | .78392 | 5+ |
| .47732 | 3+ | .80906 | 6 |
| .52077 | 3- | .88615 | 10 |
| .56544 | 1 | .92038 | 2 dif |
| .58974 | 2+ | .93188 | 2 dif |
| .61180 | 3+ | .96735 | 3 dif |

Figure 29 shows the isothermal section of the hafnium-iridium-boron ternary system at 1100°C.

An interesting characteristic of the ternary system is the somewhat extended solid solution of the $HfIr_3$ binary phase. At 1100°C the $HfIr_3$ phase takes about 15 Mole % boron into solid solution. Information from the X-ray films of some of the samples which were arc melted showed the $HfIr_3$(B) solid solution increases its range into the ternary at temperatures near its melting point and takes almost 24 Mole% boron into solution; in addition, the width of this single phase region near the boron-rich boundary

encompasses a spread of about 13 At.% hafnium and ranges from 24 to 11 At.% Hf. In a similar manner, the ternary phase $Hf_{.19}Ir_{.49}B_{.32}(T_1)$ also increases its homogeneous range considerably at temperatures near melting; the boundaries of this ternary phase at temperatures just below the solidus are given by: $Hf_{0.21 \pm .02}$ $Ir_{0.49 \pm .03}$ $B_{0.30 \pm .03}$.

Table 15 shows the variation of the lattice parameters of the $HfIr_3(B)$ solid solution with composition; also included are some lattice parameters taken from a few arc melted samples containing this phase.

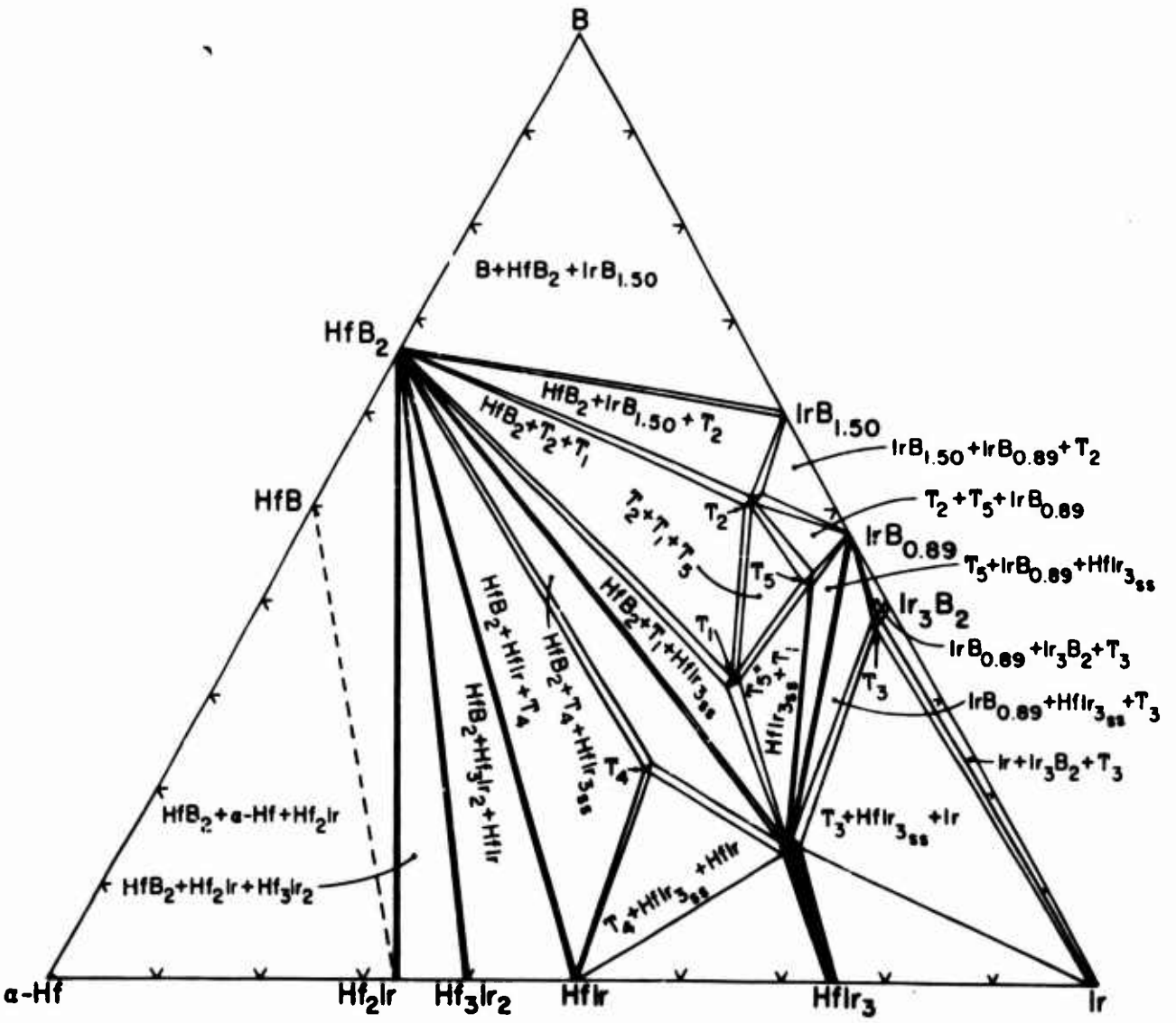


Figure 29. The Hafnium-Iridium-Boron System at 1100°C.

Table 15. Lattice Parameters of the $HfIr_3$(B) Solid Solution.

| Nominal Composition At.% | | | Lattice Parameter in Angstroms | Remarks |
|---|---|---|---|---|
| Hf | Ir | B | | |
| 26 | 69 | 5 | $3.97_4$ | Arc Melted |
| 22 | 65 | 13 | $3.99_8$ | Heat Treated-1100°C |
| 22 | 65 | 13 | $3.97_9$ | Arc Melted |
| 23 | 60 | 17 | $3.99_8$ | Heat Treated-1100°C |
| 22 | 53 | 25 | $3.98_1$ | Heat Treated-1100°C |
| 22 | 53 | 25 | $3.97_2$ | Arc Melted |
| 20 | 50 | 30 | $3.97_3$ | Arc Melted |
| 26 | 41 | 33 | $3.98_6$ | Heat Treated-1100°C |

In contrast to the $HfIr_3$ phase, the $HfB_2$ phase does not show any solubility for any of the other binary or ternary phases; no lattice parameter changes, relative to pure $HfB_2$, were noticed in ternary samples either heat treated at 1100°C or arc melted. By the same token, no solubilities into the ternary field were observed for any of the iridium borides or hafnium iridides, except $HfIr_3$.

The X-ray patterns of samples in the region $HfB_2$-$Hf_2Ir$-α-Hf showed very faint traces of a pattern which possibly corresponds to that of the HfB phase. In general, however, no definite conclusion could be drawn as to whether or not the HfB partakes of the ternary phase equilibria. In fact, the evidence obtained seems to support a previous supposition[18] that the HfB phase is not stable below 1250°C. The possible equilibrium with HfB has been drawn in as a dashed line in the isothermal section.

Ternary samples, heat treated at 1100°C, which showed phases in equilibrium with the HfIr phase, were found to contain only the simple pattern of this HfIr phase. Apparently, the HfIr phase is stabilized to lower temperatures by boron in the ternary region, whereas the two neighboring phases, $HfIr_{1+x}$ and $HfIr_{1-x}$, do not partake of the ternary phase equilibria. For the sake of clarity, only the equilibria involving the HfIr phase are depicted in the ternary isothermal section presented (Figure 29).

## V. DISCUSSION

The underlying reason for the investigation of the hafnium-iridium-boron system, or this group of (Hf, Zr)-(Platinum-Metal)-B system was to determine if either of the two refractory diborides are in equilibrium with any of the platinum metals.

Studies indicated that the equilibrium refractory boride-platinum group metal does not exist in any of the combinations with Os, Pt, Rh, or Ir.

Preceding the investigation of the ternary Hf-Ir-B system, it was necessary to study the characteristics of the two unknown binaries, Hf-Ir and Ir-B. The surprisingly very low melting points in the Ir-B system gave an indication of the low stability of the intermediate iridium borides, and also, indirectly of the behavior to be expected in the ternary system. As evidenced by the results of these investigations, due to the lack of a higher stability on the part of the iridium borides, only one, two-phased equilibrium between $HfB_2$ and the iridium-boron binary ($HfB_2$-$IrB_{1.50}$) exists; and, five ternary phases are formed. Unfortunately, no two-phased, or even three-phased, equilibrium exists with $HfB_2$ and iridium; that is, iridium cannot be used in direct combination with $HfB_2$ in a composite body for elevated temperature applications.

In fact, aside from the chemical incompatibility, the low melting temperatures of the iridium-boron binary are expected to be projected into the ternary, further limiting any elevated temperature application.

The possibility of using the $HfIr_3(B)$ solid solution as a barrier material between iridium and $HfB_2$ might be considered for certain constant, high temperature applications in as much as the $HfIr_3(B)$ solid solution is in equilibrium with both $HfB_2$ and iridium; however, a composite body employing this barrier type material construction would certainly fail over a period of time in a cycling temperature environment. The strongly temperature dependent solubility of the $HfIr_3$ phase for both boron and iridium would lead to a mechanical failure due to solutioning and precipitation of the respective components.

A re-examination of the samples in the ternary boride systems with the other metals, osmium, rhodium, and platinum with hafnium and zirconium showed that the crystal structural behavior of hafnium and zirconium was similar in all cases, as is to be expected. It was further noted that some ternary phases with rhodium were isomorphic with those observed in the ternary Hf-Ir-B system; in these combinations, rhodium and iridium appear to behave in a similar manner as far as structural chemistry is concerned. On the other hand, those ternary compounds containing platinum or osmium do not seem to show any structural chemical isomorphism, either between themselves or to iridium or rhodium phases.

The elucidation of the hafnium-iridium-boron ternary system, used in conjunction with the observed similarities of the neighboring sister elements, should assist greatly in the clarification of the other ternary systems of the (Hf, Zr)-(Plat. Met)-Boron group.

## REFERENCES


1. L. Kaufman and E.V. Clougherty: RTD-TDR-63-4096, Part II (Feb 1965).

2. M.V. Nevitt and L.H. Schwartz: Trans.AIME, October (1958), 700.

3. A.E. Dwight: Trans. AIME 215 (1959), 283.

4. A.E. Dwight and P.A. Beck: Trans. AIME 215 (1959), 976.

5. J.H. Buddery and A.J.E. Welch: Nature, 167 (1951), 362.

6. G. Reinacher: Revue de Metallurgie 54, No.5 (1957), 321.

7. B. Aronsson, E. Stenberg, and J. Åselius: Acta Chem. Scand. 14 (1960), 733.

8. B. Aronsson, J. Åselius, and E. Stenberg: Nature 183 (1959), 1318.

9. G.V. Samsonov, L. Ya.Moskovskii, A.F. Zhigach, and M.G. Valyashko: Boron, Its Compounds and Alloys, AEC-TR-5032 (Book 2), translated from a publication of the Publishing House of the Academy of Sciences of the Ukranian SSR, Kiev, (1960).

10. K. Moers: Z. anorg.allg. Chem. 198 (1931), 262.

11. F. Glaser, D. Moskowitz, and B. Post: J.Metals 5 (1953), 1119.

12. C. Agte and K. Moers: Z. anorg. allg. Chemie. 198 (1931), 233.

13. R. Kieffer, F. Benesovsky, and E. Honak: Z. anorg.allg. Chem. 268, (1952), 191.

14. E. Rudy and F. Benesovsky: Mh.Chem. 92, (1961), 415.

15. H. Nowotny, H. Braun, and F. Benesovsky: Radex-Rundsch.(1960), 367.

16. E. Rudy: Thesis, Technische Hochschule, Vienna (1960).

17. R. Kieffer and F. Benesovsky: Hartstoffe, Springer Verlag, Vienna, Austria , (1963), 396.

18. E. Rudy and St. Windisch: AFML-TR-65-2, Part I, Vol. IX., (Jan 1966).

19. E. Rudy, St. Windisch, and Y.A. Chang: AFML-TR-65-2, Part I, Vol. 1, Jan 1965

## REFERENCES (Cont'd)


20. E. Rudy and G. Progulski: AFML-TR-65-2, Part III, Vol. II, (Sep 1966)

21. E. Rudy and St. Windisch: AFML-TR-65-2, Part I, Vol. VII (Oct 1965)

Unclassified

Security Classification

**DOCUMENT CONTROL DATA - R&D**

*(Security classification of title, body of abstract and indexing annotation must be entered when the overall report is classified)*

| | |
|---|---|
| ORIGINATING ACTIVITY *(Corporate author)*<br>Aerojet-General Corporation<br>Materials Research Laboratory<br>Sacramento, California | 2a. REPORT SECURITY CLASSIFICATION<br>Unclassified<br>2b GROUP<br>N.A. |

3. REPORT TITLE

Ternary Phase Equilibria in Transition Metal-Boron-Carbon-Silicon Systems

Part II. Ternary Systems. Vol. XIV. The Hafnium-Iridium-Boron System

4. DESCRIPTIVE NOTES *(Type of report and inclusive dates)*

5. AUTHOR(S) *(Last name, first name, initial)*

Brukl, Charles E.
Rudy, Erwin

| 6. REPORT DATE | 7a. TOTAL NO. OF PAGES | 7b. NO. OF REFS |
|---|---|---|
| July 1967 | 54 | 21 |

| | |
|---|---|
| 8a. CONTRACT OR GRANT NO. AF 33(615)-1249<br>b. PROJECT NO. 7350<br>c. Task No. 735001<br>d. | 9a. ORIGINATOR'S REPORT NUMBER(S)<br>AFML-TR-65-2<br>Part II, Vol. XIV<br>9b. OTHER REPORT NO(S) *(Any other numbers that may be assigned this report)*<br>N.A. |

10. AVAILABILITY/LIMITATION NOTICES

This document is subject to special export controls, and each transmittal to foreign governments or foreign nationals may be made only with prior approval of Metals & Ceramics Div., AF Materials Lab., Wright-Patterson AFB, Ohio.

| 11. SUPPLEMENTARY NOTES | 12. SPONSORING MILITARY ACTIVITY |
|---|---|
| | AFML (MAMC)<br>Wright-Patterson AFB, Ohio 45433 |

13. ABSTRACT


Constitution diagrams of the binary hafnium-iridium and iridium-boron systems as well as an isothermal section of the hafnium-iridium-boron ternary system have been established by means of Pirani melting point investigations, metallography, Debye-Scherrer X-ray, and chemical analysis.

There are three intermediate phases, $Ir_3B_2$, $IrB_{0.89}$, and $IrB_{1.60}$ in the rather low melting iridium-boron system which contains four eutectics.

$Hf_2Ir$, $Hf_3Ir_2$, $HfIr_{1-x}$, HfIr, $HfIr_{1-x}$, and $HfIr_3$ are the phases present in the hafnium-iridium system. The highest melting phase in this system is $HfIr_3$ whose melting point is 2460°C. The phase relationships in the central portion of the binary system are quite complex.

The ternary hafnium-iridium-boron system has five ternary phases: $Hf_{.32}Ir_{.46}B_{.22}$, $Hf_{.19}Ir_{.49}B_{.32}$, $Hf_{.07}Ir_{.51}B_{.42}$, $Hf_{.07}Ir_{.42}B_{.51}$, and $Hf_{.02}Ir_{.60}B_{.38}$. $HfIr_3$ has an extended solubility for boron. $HfB_2$, which does not form a two-phase equilibrium with iridium, exhibits no solubility into the ternary field.

High temperature application possibilities for hafnium-iridium-boron composite borides are briefly discussed.


DD FORM 1 JAN 64 1473

Unclassified

Security Classification

Unclassified

Security Classification

| 14. KEY WORDS | LINK A | | LINK B | | LINK C | |
|---|---|---|---|---|---|---|
| | ROLE | WT | ROLE | WT | ROLE | WT |
| Binary Phase Equilibria<br>Ternary Phase Equilibria<br>Hafnium-Iridium<br>Iridium-Boron<br>Hafnium-Iridium-Boron | | | | | | |

## INSTRUCTIONS

1. ORIGINATING ACTIVITY: Enter the name and address of the contractor, subcontractor, grantee, Department of Defense activity or other organization *(corporate author)* issuing the report.

2a. REPORT SECURITY CLASSIFICATION: Enter the overall security classification of the report. Indicate whether "Restricted Data" is included. Marking is to be in accordance with appropriate security regulations.

2b. GROUP: Automatic downgrading is specified in DoD Directive 5200.10 and Armed Forces Industrial Manual. Enter the group number. Also, when applicable, show that optional markings have been used for Group 3 and Group 4 as authorized.

3. REPORT TITLE: Enter the complete report title in all capital letters. Titles in all cases should be unclassified. If a meaningful title cannot be selected without classification, show title classification in all capitals in parenthesis immediately following the title.

4. DESCRIPTIVE NOTES: If appropriate, enter the type of report, e.g., interim, progress, summary, annual, or final. Give the inclusive dates when a specific reporting period is covered.

5. AUTHOR(S): Enter the name(s) of author(s) as shown on or in the report. Enter last name, first name, middle initial. If military, show rank and branch of service. The name of the principal author is an absolute minimum requirement.

6. REPORT DATE: Enter the date of the report as day, month, year; or month, year. If more than one date appears on the report, use date of publication.

7a. TOTAL NUMBER OF PAGES: The total page count should follow normal pagination procedures, i.e., enter the number of pages containing information.

7b. NUMBER OF REFERENCES: Enter the total number of references cited in the report.

8a. CONTRACT OR GRANT NUMBER: If appropriate, enter the applicable number of the contract or grant under which the report was written.

8b, 8c, & 8d. PROJECT NUMBER: Enter the appropriate military department identification, such as project number, subproject number, system numbers, task number, etc.

9a. ORIGINATOR'S REPORT NUMBER(S): Enter the official report number by which the document will be identified and controlled by the originating activity. This number must be unique to this report.

9b. OTHER REPORT NUMBER(S): If the report has been assigned any other report numbers *(either by the originator or by the sponsor)*, also enter this number(s).

10. AVAILABILITY/LIMITATION NOTICES: Enter any limitations on further dissemination of the report, other than those imposed by security classification, using standard statements such as:

(1) "Qualified requesters may obtain copies of this report from DDC."

(2) "Foreign announcement and dissemination of this report by DDC is not authorized."

(3) "U. S. Government agencies may obtain copies of this report directly from DDC. Other qualified DDC users shall request through

_____."

(4) "U. S. military agencies may obtain copies of this report directly from DDC. Other qualified users shall request through

_____."

(5) "All distribution of this report is controlled. Qualified DDC users shall request through

_____."

If the report has been furnished to the Office of Technical Services, Department of Commerce, for sale to the public, indicate this fact and enter the price, if known.

11. SUPPLEMENTARY NOTES: Use for additional explanatory notes.

12. SPONSORING MILITARY ACTIVITY: Enter the name of the departmental project office or laboratory sponsoring *(paying for)* the research and development. Include address.

13. ABSTRACT: Enter an abstract giving a brief and factual summary of the document indicative of the report, even though it may also appear elsewhere in the body of the technical report. If additional space is required, a continuation sheet shall be attached.

It is highly desirable that the abstract of classified reports be unclassified. Each paragraph of the abstract shall end with an indication of the military security classification of the information in the paragraph, represented as *(TS), (S), (C), or (U)*.

There is no limitation on the length of the abstract. However, the suggested length is from 150 to 225 words.

14. KEY WORDS: Key words are technically meaningful terms or short phrases that characterize a report and may be used as index entries for cataloging the report. Key words must be selected so that no security classification is required. Identifiers, such as equipment model designation, trade name, military project code name, geographic location, may be used as key words but will be followed by an indication of technical context. The assignment of links, rules, and weights is optional.

Unclassified

Security Classification